endoscopy should be biopsied to determine the diagnosis and further treatment.

Key words: Biopsy; Minute pharyngeal lesions; Narrow-band imaging

Peer reviewers: Hoon Jai Chun, MD, PhD, AGAF, Professor, Department of Internal Medicine, Institute of Digestive Disease and Nutrition, Korea University College of Medicine, 126-1, Anam-dong 5-ga, Seongbuk-gu, Seoul 136-705, South Korea; Hiroki Nakamura, MD, Department of Gastroenterology and Hepatology, 1-1-1, Minami Kogushi, Ube, Yamaguchi 755-8505, Japan

Kumamoto T, Sentani K, Oka S, Tanaka S, Yasui W. Clinicopathological features of minute pharyngeal lesions diagnosed by narrow-band imaging endoscopy and biopsy. *World J Gastroenterol* 2012; 18(44): 6468-6474 Available from: URL: http://www.wjgnet.com/1007-9327/full/v18/i44/6468.htm DOI: http://dx.doi.org/10.3748/wjg.v18.i44.6468

INTRODUCTION

Magnified narrow-band imaging (NBI) endoscopy is reportedly useful for early pharyngeal[1-5] and esophageal cancer diagnosis[6-10]. Magnified NBI is useful both for detecting suspicious changes and for further diagnostic purposes, such as determining whether a lesion is suspected of being dysplasia or cancer[11,12]. We routinely examined upper gastrointestinal tracts using magnified NBI for one and a half years. When the unmagnified NBI detected a brownish area in the pharynx, a magnified NBI examination was used to aid the intrapapillary capillary loop (IPCL) classification[12-14]. If IPCL type Ⅳ or Ⅴ was observed, dysplasia or cancer was suspected, and treatment was considered. Although endoscopic submucosal dissection (ESD) leads to complete resection, ESD is an inpatient procedure that requires intubation anesthesia. For smaller (approximately 1 mm) lesions, therefore, our first choice is to biopsy the lesion for histological diagnosis while performing a complete resection. There have been no previous reports on the utility of biopsying minute pharyngeal lesions. This article reports our histological diagnosis, treatment, and follow-up findings from minute pharyngeal dysplasia biopsies.

MATERIALS AND METHODS

Patients

Most patients over 30 years old who require gastrointestinal endoscopy at the clinic are examined by magnified NBI. From August 2008 to March 2010, a total of 93 consecutive patients with IPCL type Ⅳ pharyngeal lesions, as determined by magnified NBI, were enrolled in this study (Table 1). The patients included 80 men aged 39-87 years (mean age, 66.9 years) and 13 women aged 43-84 years (mean age, 67.1 years). Drinking and smoking habits were assessed for 86 patients. Lesions of approximately 1 mm in diameter were found in 62 patients and were biopsied at the clinic, and the 17 patients with larger lesions were endoscopically resected by ESD at the Hiroshima University Hospital. Detailed histological assessments were performed for 62 of the biopsies. Thirty-four of the 62 biopsied patients received follow up endoscopy.

Instruments

The following instruments were used in this study: a magnifying endoscope that was capable of × 80 magnification (GIF H260Z; Olympus Optical Co. Ltd, Tokyo, Japan), a standard videoendoscopy system (EVIS LUCERA; Olympus), and an NBI system (Olympus).

Endoscopic examination

All of the endoscopic examinations were performed by the first author (Kumamoto T). A magnification hood (MB-46, Olympus) was attached to the tip of the endoscope. Intravenous access and pulse oximetry monitoring were established prior to the examination. Most of the examinations were performed under intravenous pethidine hydrochloride (17.5-70 mg) and midazolam (0.5-4 mg) sedation. The pharynx was mainly observed by NBI from the beginning of the examination. The pharynx was examined in the following order: uvula, posterior oropharyngeal wall, epiglottis, posterior hypopharyngeal wall, and pyriform sinus. The pharynx observation time was approximately 1 min. Magnified NBI was used for all pharynx lesions with noticeable brownish areas in the NBI examination, and an IPCL classification was performed. The IPCL classification followed the criteria of Dr. Inoue H[12,13]. According to these criteria, a lesion must meet three of the following four characteristics to be classified as IPCL type Ⅳ: dilatation, tortuous running, caliber changes, and different shapes in each IPCL[12-14]. In the 93 IPCL type Ⅳ lesions, smaller lesions of approximately 1 mm in diameter were biopsied with disposable biopsy forceps (FB-210K, Olympus). To avoid post-biopsy bleeding, all anticoagulants were discontinued from 3 d before to 3 d after the biopsy. The biopsy patients remained in the clinic for 2-3 h, including a 1 h post-sedation recovery time. Annual magnified NBI examinations were recommended to all of the biopsy patients, and 34 of 62 biopsy patients received follow up. To reduce inter-observer variation, the results of the NBI and magnified NBI examinations were independently evaluated by 2 endoscopy examiners (Kumamoto T and Oka S). When the evaluations differed, a consensus decision was achieved by reviewing the magnified NBI images.

Histological methods and criteria for pathological diagnosis

The biopsy specimens were extended and fixed to a styrene foam plate by fine acupuncture needles. All of the specimens were fixed in 10% formalin and embedded in

Table 1 Patient characteristics (n = 93)

Characteristics	No.
Age, yr (range)	67 (39-87)
Sex, men/women	80/13
Alcohol consumption	
Yes	56 (54 men, 2 women)
No	30 (22 men, 8 women)
Smoker	
Yes	57 (56 men, 1 woman)
No	29 (20 men, 9 women)
Esophageal cancer history	
Yes	2
No	91
Other cancer history	
Yes	9 (8 gastric cancer, 1 colon cancer)
No	84
Location	
Hypopharynx	21 (17 men, 4 women)
Oropharynx	72 (63 men, 9 women)
Biopsy cases	62
High-grade dysplasia	3
Low-grade dysplasia	25
Non-dysplasia	34
ESD cases	17
High-grade dysplasia	2
Low-grade dysplasia	14
Non-dysplasia	1

ESD: Endoscopic submucosal dissection.

Table 2 Histological characteristics of the biopsied pharyngeal lesions n (%)

	Non-D	LGD	HGD
Number	34	25	3
IPCL			
Upward extension	26 (76)	24 (96)	3 (100)
Dilatation and branching	5 (15)	21 (84)	3 (100)
Diameter expansion	0 (0)	8 (25)	1 (33)
Architectural atypia			
Proliferative cell distribution			
≥ 2/3	0 (0)	0 (0)	3 (100)
< 2/3	34 (100)	25 (100)	0 (0)
Tumor front	0 (0)	23 (92)	3 (100)
Cytological atypia			
Abnormal variation in cell size	0 (0)	2 (8)	3 (100)
Abnormal nuclear arrangement	0 (0)	23 (92)	3 (100)
Increased nuclear size			
High	0 (0)	0 (0)	3 (100)
Absent or low	34 (100)	25 (100)	0 (0)

Non-D: Non-dysplastic; LGD: Low-grade dysplasia; HGD: High-grade dysplasia; IPCL: Intra-papillary capillary loop.

paraffin wax. The tissue specimens were cut into 3-μm thick sections, and all of the sections received routine pathological diagnoses. The pathological parameters of each lesion were independently evaluated by two pathologists (Sentani K, Yasui W) and used for further analyses. The dysplasia diagnoses followed the criteria proposed by the World Health Organization[15]. In this study, dysplasia was classified as low-grade (mild or moderate dysplasia) or high-grade (severe dysplasia). These criteria were based on the architectural and cytological abnormalities. In addition to these abnormalities, IPCL changes were considered[16]. As shown in Table 2, the histological diagnoses were based on the IPCL changes and on architectural and cytological atypia. The IPCL changes were defined as upward extension, dilatation and branching, and diameter expansion. Architectural atypia was determined by a proliferative cell distribution and the tumor front, and cytological atypia was assessed by cell size, nuclear arrangement and nuclear size. The lesion diameters were measured under light microscopy using the built-in measurement system of the light microscope, which measured to an accuracy of 0.1 mm.

RESULTS

Minute pharyngeal lesions were diagnosed in 93 of approximately 3000 patients who were examined by magnified NBI. The clinicopathological characteristics of the patients are shown in Table 1. Of the 93 patients, 80 were men, and 13 were women. Fifty-six patients were drinkers, 57 were smokers, and 2 had esophageal cancer. Other cancers included gastric cancer in 8 patients and colon cancer in 1 patient. Twenty-one lesions were located on the posterior hypopharyngeal wall, and 72 lesions were found on the posterior oropharyngeal wall.

All 93 lesions were flat and showed similar findings in the magnified and unmagnified NBI examinations (Figures 1B, C; 2A, B). Most of the IPCL type Ⅳ lesions were identifiable immediately after the magnified NBI diagnosis by a faint redness under white light (Figure 1A). However, it was difficult to diagnose IPCL type Ⅳ lesions by this characteristic before an NBI examination because the contrast is weaker than that of NBI (Figure 1A, B). Of the 93 lesions, only 3 were greater than 2.1 mm in diameter, and the remaining lesions were less than 2.0 mm in diameter. Sixty-two lesions of approximately 1 mm in diameter were biopsied for histological diagnoses at the clinic, and 17 larger lesions were treated by ESD at the Hiroshima University Hospital. There were no complications, such as bleeding or pharyngeal pain, during or after the ESD.

The histological diagnoses of the 79 lesions resected by biopsy or ESD included 5 cases of high-grade dysplasia, 39 cases of low-grade dysplasia, and 35 non-dysplastic lesions. The 35 non-dysplastic cases consisted of 19 inflamed (pharyngitis) and 16 normal lesions. A lesion diagnosed as high-grade dysplasia is shown in Figure 1, and an example of low-grade dysplasia is shown in Figure 2. There were no cancerous lesions. The histological features of each type of dysplasia are shown in Table 2. In high-grade dysplasia, the polarity of the nucleus was lost, and the nuclear density was markedly increased throughout the intraepithelial layer, although the superficial portion of the epithelium was mature (Figure 1E). The microvascular irregularities were more severe than those seen in low-grade dysplasia. Basal cell palisading was observed in the low-grade dysplasia lesions; however, proliferative cells with enlarged nuclei that proliferated

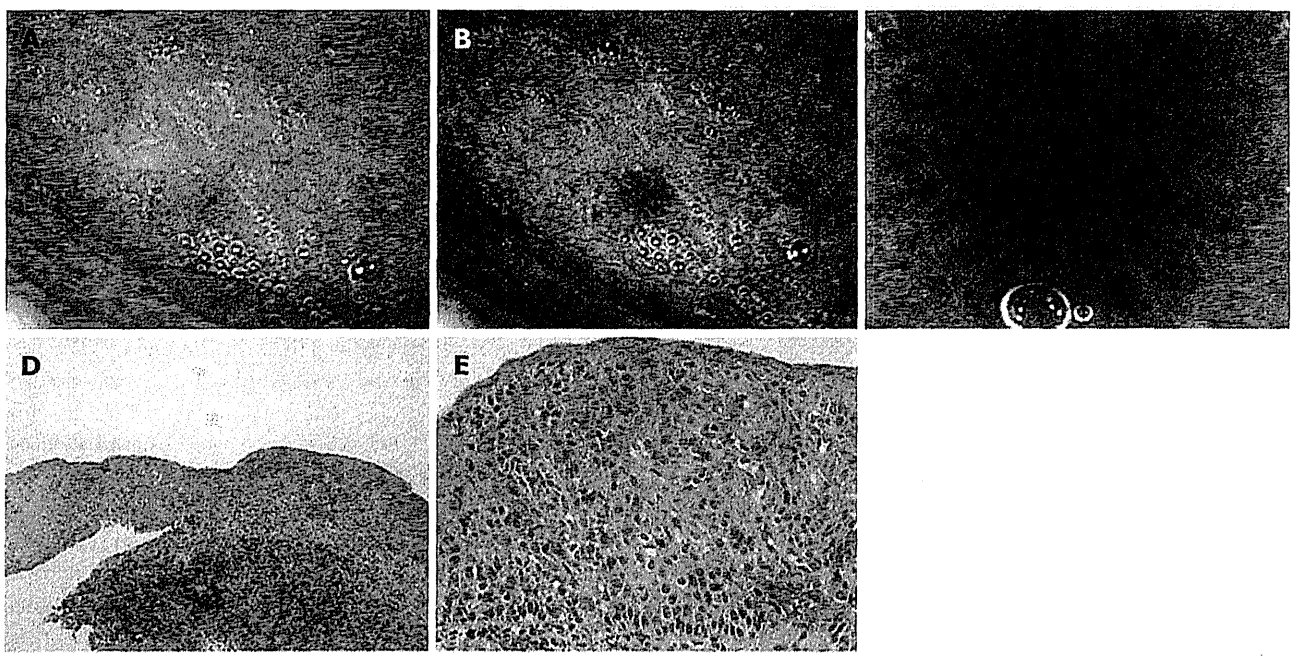

Figure 1 Narrow-band imaging view and histological image of high-grade dysplasia. A: An endoscopic photograph showing an oropharynx with high-grade dysplasia. The slightly reddish colored mucosa is the dysplastic lesion; B: The narrow-band imaging (NBI) corresponding to A, showing a well-demarcated brownish area; C: The magnified NBI view, showing an intra-papillary capillary loop type Ⅳ pattern. Irregular morphological changes in the superficial microvessels can be observed in the brownish area; D: Low-power magnification of the biopsied specimen, showing tumor front formation and complete epithelial layer invasion. The diameter of the lesion was 1.1 mm [hematoxylin and eosin (HE), original × 100]; E: Histologically, the lesion showed abnormal cell size variation and increased nuclear size; it was diagnosed as high-grade dysplasia (HE, original × 400).

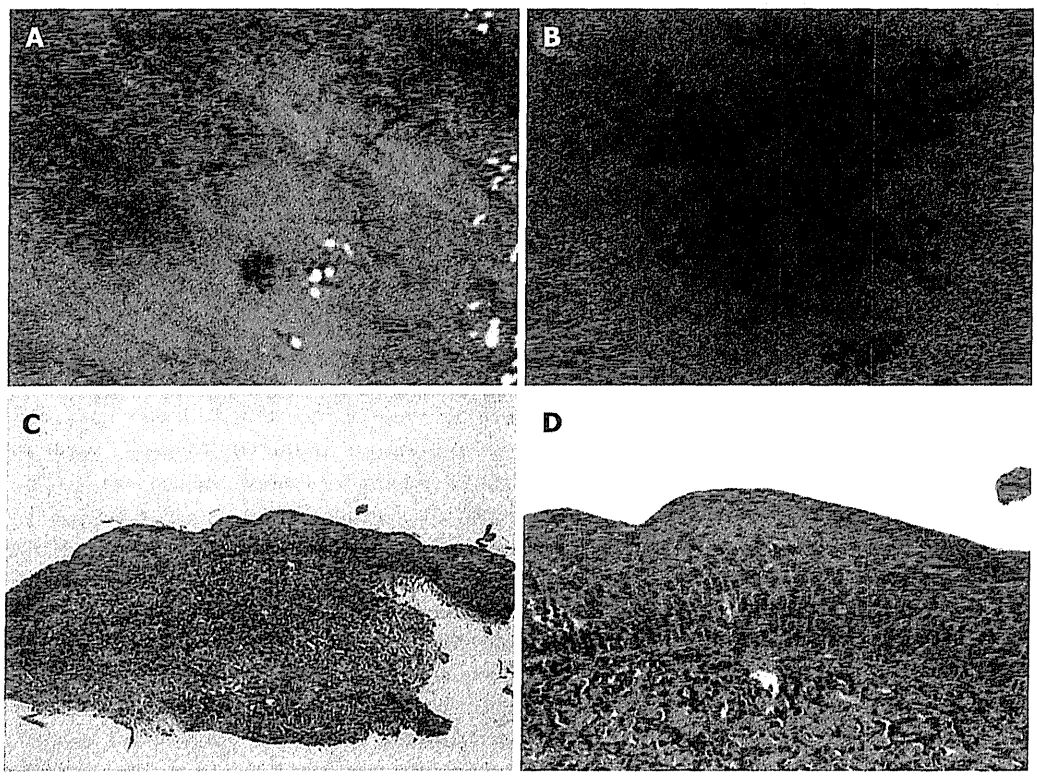

Figure 2 Narrow-band imaging view and histological image of low-grade dysplasia. A: Narrow-band imaging (NBI) showing the oropharynx with a well-demarcated brownish area; B: A magnified NBI magnifying view showing an intra-papillary capillary loop type Ⅳ pattern; C: Low power magnification of the biopsied specimen [hematoxylin and eosin (HE), original ×100]; D: Histologically, the lesion showed minimal cell size variation and was diagnosed as low-grade dysplasia (HE, original × 400).

Table 3 Diameters of the biopsied lesions *n* (%)

Diameter (mm)	*n*	Non-D	LGD	HGD
0.1-0.2	3	3 (100)	0 (0)	0 (0)
0.3-0.4	5	3 (60)	2 (40)	0 (0)
0.5-0.6	5	4 (80)	1 (20)	0 (0)
0.7-0.8	10	6 (60)	4 (40)	0 (0)
0.9-1.0	7	2 (29)	4 (57)	1 (14)
1.1-1.2	9	1 (11)	7 (78)	1 (11)
1.3-1.4	2	0 (0)	1 (50)	1 (50)
1.5-1.8	1	0 (0)	1 (100)	0 (0)
1.9-2.0	3	0 (0)	3 (100)	0 (0)

Non-D: Non-dysplasia; LGD: Low-grade dysplasia; HGD: High-grade dysplasia.

in a lamellar pattern were limited to the lower two-thirds of the epithelial layer (Figure 2D). IPCL abnormalities such as upward extension, dilatation, and diameter expansion were clearly recognized. In the high-grade dysplasia lesions, abnormal variations in cell size and increased nuclear size were observed in all of the lesions, whereas the incidence of these findings in the low-grade dysplasia lesions was low (Figures 1E, 2D). In the non-dysplastic lesions, such as inflamed squamous epithelium, intercellular edema and intraepithelial inflammatory cells were recognizable.

Of the 62 biopsied lesions, 45 were measurable (Table 3). The measured diameters were 0.1-2.0 mm (average, 1.12 mm); 30 lesions were 0.1-1.0 mm in diameter, and 15 lesions were 1.1-2.0 mm in diameter. The distribution of the lesion diameters and the neoplasia ratios are shown in Table 3. The dysplasia ratios (low-grade or high-grade) were 0% less than 0.2 mm, 20%-40% from 0.3 to 0.8 mm, 71% from 0.9 to 1.0 mm, 89% from 1.1 to 1.2 mm, and 100% from 1.3 to 2.0 mm. The ratio increased as the diameter increased. The diameters of the 3 high-grade lesions were 1.0, 1.1, and 1.3 mm.

Twenty-seven of the 34 biopsy patients who received endoscopic follow up (79%) had no lesions at the biopsy site in their NBI examinations, and complete resection from the biopsy was expected in these patients. The interval from the first diagnosis to the follow-up ranged from 4-22 mo (mean, 12.5 mo). The diameters of the lesions in the 3 incomplete resection cases were 0.7 mm, 1.1 mm, and 1.1 mm. Sixteen of the 34 cases were of high- or low-grade dysplasia, and 13 of these 16 cases (81%) had no lesions at the biopsy site. Complete resection from the biopsy was expected in these cases. The largest lesion for which complete resection was expected was 1.9 mm in diameter and was classified as low-grade dysplasia.

DISCUSSION

Magnified NBI endoscopy is preferable for diagnosing minute pharyngeal lesions[17-21]. The current practice at our clinic is to observe the pharynx and esophagus by NBI from the beginning of the examination. A distal magnification attachment on the endoscope tip is effective for quick focusing. The typical time for a magnified NBI examination from the pharynx to the duodenum was 10-15 min. The routine pharynx examination time was approximately 1 min.

During the period from September 2008 to March 2010, 93 patients with minute pharyngeal IPCL type Ⅳ lesions of approximately 1 mm in diameter were diagnosed at our clinic by magnified NBI endoscopy. During this period, we performed approximately 3000 routine examinations of the upper gastrointestinal tract using magnified NBI endoscopy. Thus, the frequency of such lesions was approximately 3%. Although it is well known that male drinkers and smokers aged over 50 are at high risk for pharyngeal carcinoma[22], we also observed several cases of low-grade dysplasia in women, and the youngest case was a 39-year-old man. Therefore, we routinely examine almost all men and women over 30 with magnified NBI endoscopy. In the present study, 2 patients had esophageal cancer[23-26], 8 had gastric cancer, and one had colon cancer. A history of other cancers may also be considered a risk factor.

All 93 lesions were intraepithelial flat lesions. Because the magnified NBI endoscopy findings were similar and showed no clear differences among high-grade dysplasia, low-grade dysplasia and non-dysplastic lesions, the 93 lesions appeared to have similar characteristics. If the lesions had been followed for a longer period, transitions from low-grade to high-grade dysplasia might have occurred. There is controversy over whether such lesions should be followed, biopsied, or treated. Because the histological diagnosis for 3 biopsied cases and 2 ESD cases was high-grade dysplasia, at least 5 lesions (all of which were in men) were considered to be precancerous. Although there were no cancerous lesions in this series[18], routinely using magnified NBI endoscopy seemed effective for diagnosing pharyngeal precancerous lesions early and showed that IPCL type Ⅳ lesions should be biopsied or resected by ESD. Because esophageal IPCL type Ⅳ lesions are thought to represent high-grade dysplasia, treatment is recommended[13]. However, treating smaller esophageal or pharyngeal IPCL type Ⅳ lesions (approximately 1 mm in diameter) is still controversial. Whether they should be treated or followed remains to be determined. Because the smaller pharyngeal IPCL type Ⅳ lesions in our study contained some precancerous lesions, we recommend biopsy and treatment over follow up.

A survey of the diameters of the biopsied lesions indicated an increase in the dysplasia ratio as the diameter increased, and all lesions over 1.3 mm were found to be dysplastic. Our clinic sees typical outpatients with varied gastrointestinal symptoms or abnormal gastric X-ray findings, and the diameter distribution we observed appears to be close to the natural distribution of such lesions. The diameter of the 3 high-grade lesions ranged from 1.0 to 1.3 mm; therefore, it would appear that lesions greater than 1.0 mm in diameter should be resected by biopsy or ESD. Furthermore, because low-grade lesions as small as 0.3 mm in diameter were observed, it would be better to

resect all lesions less than 1.0 mm in diameter. The diameter distribution appears to show the natural progression from low-grade to high-grade dysplasia.

A follow-up study of the biopsied cases revealed that the resection rate by biopsy alone was 79%. The diameter of the largest resected lesion was 1.9 mm. Although annual endoscopic follow-up must be continued, biopsy may lead to complete resection in some cases and can be performed as a first-line therapy. Single-use disposable biopsy forceps were used to obtain a biopsy specimen as large and as deep as possible for complete resection. For the biopsy, the plane of the opened biopsy forceps should be horizontal, which can be achieved by rotating the handle. Precise, lesion-centered biopsies of 1 mm lesions are difficult[13] and require high levels of concentration and cooperation between the examiner and the assisting medical staff. Recently, we have biopsied these lesions prior to inserting the endoscope into the esophagus because if we try to biopsy during the final withdrawal stage, the observations may be disturbed by secreted mucus and minute bleeding. Biopsying the pharynx appeared to be safe providing all anticoagulant drugs were discontinued from 3 d before to 3 d after biopsy. We experienced no complications (such as bleeding) after the biopsies.

Compared to the esophagus, the pharynx is sensitive to being touched by an endoscope. Therefore, almost all of the magnified NBI magnifying examinations were performed under sedation. The hypopharynx is particularly sensitive. Without sedation, the pharyngeal reflex causes responsive artificial bleeding, particularly when touched by the distal attachment during examination, and NBI observation becomes difficult due to the brownish color change in the entire endoscopic field. In our experience, magnified NBI endoscopy can be routinely performed with the patient under sedation. However, because deep sedation may cause respiratory depression, sedation should be used cautiously with an intravenous drip, and with oxygen and the counteracting effect of flumazenil readily available. In high-risk patients, such as those with respiratory or heart disease, for safety, we removed the distal attachment on the scope tip or changed the scope to a smaller diameter non-magnifying scope (GIF H260, Olympus).

In conclusion, magnified NBI endoscopy appears to be preferable for diagnosing pharyngeal neoplasia. Biopsy was useful for the diagnosis and treatment of minute pharyngeal neoplasia.

COMMENTS

Background

It has been difficult to diagnose an early-stage pharyngeal carcinoma. Narrow-band imaging (NBI) has enabled more accurate diagnosis and increased the detection rate of superficial pharyngeal carcinomas. Magnified NBI endoscopy is quite effective for diagnosing early-stage pharyngeal and esophageal carcinoma, that is, carcinomas in the squamous cell regions. The intrapapillary capillary loop (IPCL) classification for magnified NBI endoscopy is applicable only to the squamous cell regions, that is, the pharynx and the esophagus. Magnified NBI endoscopy for the stomach and the colon is evaluated by different diagnostic classifications.

Research frontiers

Magnified NBI endoscopy made it possible to diagnose minute pharyngeal lesions with diameters of approximately 1 mm. It includes two steps. First, using NBI endoscopy without magnification, the authors detected suspicious changes as brownish areas. Second, using NBI magnifying of the brownish areas, the authors were able to diagnose whether the changes were suspicious of dysplasia or cancer or not according to the IPCL classification. IPCL type IV or V shows the possibility of dysplasia or cancer, whereas IPCL type I neglects the possibility.

Innovations and breakthroughs

For larger pharyngeal IPCL type IV lesions over 10 mm diameter, endoscopic submucosal dissection (ESD) is recommended. However, for smaller lesions of approximately 1 mm diameter, it remains to be determined whether they should be resected by ESD or followed up. Studies on the biopsy of such lesions are few. The authors concluded that biopsy can be the first-line procedure for such lesions not only for diagnosis but also for treatment.

Applications

The NBI system and magnifying endoscope are necessary to begin magnified NBI endoscopy. As the pharynx is sensitive, magnified NBI endoscopy of the pharynx should be performed under sedation. For safety, sedation should be carried out cautiously. As several biopsied minute pharyngeal lesions were high grade dysplasia, minute pharyngeal lesions should be biopsied for diagnosis. Furthermore, follow-up study of the biopsied lesions showed that even complete resection was expected by biopsy.

Terminology

NBI: NBI is a new image-enhanced optical technology that uses narrow band NBI filters; IPCL: IPCL is the microvascular tumor vessel classification system used for NBI magnifying endoscopy.

Peer review

Recently it has been reported that NBI can be useful in the early detection of superficial pharyngeal cancer. To determine the criteria of endoscopic treatment in patients with pharyngeal cancer and dysplasia, the resected specimen and follow up data are required. It is a good idea to investigate the usefulness of NBI magnifying endoscopy in the pharynx because biopsy in the pharynx is difficult.

REFERENCES

1 **Nonaka S**, Saito Y. Endoscopic diagnosis of pharyngeal carcinoma by NBI. *Endoscopy* 2008; **40**: 347-351

2 **Muto M**, Nakane M, Katada C, Sano Y, Ohtsu A, Esumi H, Ebihara S, Yoshida S. Squamous cell carcinoma in situ at oropharyngeal and hypopharyngeal mucosal sites. *Cancer* 2004; **101**: 1375-1381

3 **Ugumori T**, Muto M, Hayashi R, Hayashi T, Kishimoto S. Prospective study of early detection of pharyngeal superficial carcinoma with the narrowband imaging laryngoscope. *Head Neck* 2009; **31**: 189-194

4 **Watanabe A**, Tsujie H, Taniguchi M, Hosokawa M, Fujita M, Sasaki S. Laryngoscopic detection of pharyngeal carcinoma in situ with narrowband imaging. *Laryngoscope* 2006; **116**: 650-654

5 **Matsuba H**, Katada C, Masaki T, Nakayama M, Okamoto T, Hanaoka N, Tanabe S, Koizumi W, Okamoto M, Muto M. Diagnosis of the extent of advanced oropharyngeal and hypopharyngeal cancers by narrow band imaging with magnifying endoscopy. *Laryngoscope* 2011; **121**: 753-759

6 **Yoshida T**, Inoue H, Usui S, Satodate H, Fukami N, Kudo SE. Narrow-band imaging system with magnifying endoscopy for superficial esophageal lesions. *Gastrointest Endosc* 2004; **59**: 288-295

7 **Muto M**, Minashi K, Yano T, Saito Y, Oda I, Nonaka S, Omori T, Sugiura H, Goda K, Kaise M, Inoue H, Ishikawa H, Ochiai A, Shimoda T, Watanabe H, Tajiri H, Saito D. Early detection of superficial squamous cell carcinoma in the head and neck region and esophagus by narrow band imaging: a multicenter randomized controlled trial. *J Clin Oncol* 2010;

28: 1566-1572

8 **Muto M**, Hironaka S, Nakane M, Boku N, Ohtsu A, Yoshida S. Association of multiple Lugol-voiding lesions with synchronous and metachronous esophageal squamous cell carcinoma in patients with head and neck cancer. *Gastrointest Endosc* 2002; **56**: 517-521

9 **Muto M**, Takahashi M, Ohtsu A, Ebihara S, Yoshida S, Esumi H. Risk of multiple squamous cell carcinomas both in the esophagus and the head and neck region. *Carcinogenesis* 2005; **26**: 1008-1012

10 **Muto M**, Katada C, Sano Y, Yoshida S. Narrow band imaging: a new diagnostic approach to visualize angiogenesis in superficial neoplasia. *Clin Gastroenterol Hepatol* 2005; **3**: S16-S20

11 **Muto M**, Ugumori T, Sano Y, Ohtsu A. Yoshida S. Narrow-band imaging combined with magnified endoscopy for cancer at the head and neck region. *Dig Endosc* 2005; **17**: S23-S24

12 **Inoue H**. Magnification endoscopy in the esophagus and stomach. *Dig Endosc* 2001; **13**: S40-S41

13 **Inoue H**, Kaga M, Sato Y, Sugaya S, Kudo S. Magnifying endoscopic diagnosis of tissue atypia and cancer invasion depth in the area of pharyngo-esophageal squamous epithelium by NBI enhanced magnification image: IPCL pattern classification. In: Cohen J. Advanced Digestive Endoscopy: Comprehensive Atlas of High Resolution Endoscopy and Narrowband Imaging. Oxford: Wiley-Blackwell, 2007:49-66

14 **Kumagai Y**, Inoue H, Nagai K, Kawano T, Iwai T. Magnifying endoscopy, stereoscopic microscopy, and the microvascular architecture of superficial esophageal carcinoma. *Endoscopy* 2002; **34**: 369-375

15 **Barnes L**, Eveson JW, Reichart P, Sidransky D (Eds): World Health Organization Classification of Tumours. Pathology and Genetics of Head and Neck Tumours. Lyon: IARC Press, 2005

16 **Fujii S**, Yamazaki M, Muto M, Ochiai A. Microvascular irregularities are associated with composition of squamous epithelial lesions and correlate with subepithelial invasion of superficial-type pharyngeal squamous cell carcinoma. *Histopathology* 2010; **56**: 510-522

17 **Yoshimura N**, Goda K, Tajiri H, Yoshida Y, Kato T, Seino Y, Ikegami M, Urashima M. Diagnostic utility of narrow-band imaging endoscopy for pharyngeal superficial carcinoma. *World J Gastroenterol* 2011; **17**: 4999-5006

18 **Tanaka S**, Morita Y, Fujita T, Yokozaki H, Obata D, Fujiwara S, Wakahara C, Masuda A, Sugimoto M, Sanuki T, Yoshida M, Toyonaga T, Kutsumi H, Azuma T. Clinicopathological characteristics of abnormal micro-lesions at the oro-hypopharynx detected by a magnifying narrow band imaging system. *Dig Endosc* 2012; **24**: 100-109

19 **Shimizu Y**, Tsukagoshi H, Fujita M, Hosokawa M, Watanabe A, Kawabori S, Kato M, Sugiyama T, Asaka M. Head and neck cancer arising after endoscopic mucosal resection for squamous cell carcinoma of the esophagus. *Endoscopy* 2003; **35**: 322-326

20 **Katada C**, Nakayama M, Tanabe S, Koizumi W, Masaki T, Takeda M, Okamoto M, Saigenji K. Narrow band imaging for detecting metachronous superficial oropharyngeal and hypopharyngeal squamous cell carcinomas after chemoradiotherapy for head and neck cancers. *Laryngoscope* 2008; **118**: 1787-1790

21 **Katada C**, Tanabe S, Koizumi W, Higuchi K, Sasaki T, Azuma M, Katada N, Masaki T, Nakayama M, Okamoto M, Muto M. Narrow band imaging for detecting superficial squamous cell carcinoma of the head and neck in patients with esophageal squamous cell carcinoma. *Endoscopy* 2010; **42**: 185-190

22 **Yokoyama A**, Kato H, Yokoyama T, Tsujinaka T, Muto M, Omori T, Haneda T, Kumagai Y, Igaki H, Yokoyama M, Watanabe H, Fukuda H, Yoshimizu H. Genetic polymorphisms of alcohol and aldehyde dehydrogenases and glutathione S-transferase M1 and drinking, smoking, and diet in Japanese men with esophageal squamous cell carcinoma. *Carcinogenesis* 2002; **23**: 1851-1859

23 **Morita M**, Kuwano H, Ohno S, Sugimachi K, Seo Y, Tomoda H, Furusawa M, Nakashima T. Multiple occurrence of carcinoma in the upper aerodigestive tract associated with esophageal cancer: reference to smoking, drinking and family history. *Int J Cancer* 1994; **58**: 207-210

24 **Nonaka S**, Saito Y, Oda I, Kozu T, Saito D. Narrow-band imaging endoscopy with magnification is useful for detecting metachronous superficial pharyngeal cancer in patients with esophageal squamous cell carcinoma. *J Gastroenterol Hepatol* 2010; **25**: 264-269

25 **Matsubara T**, Yamada K, Nakagawa A. Risk of second primary malignancy after esophagectomy for squamous cell carcinoma of the thoracic esophagus. *J Clin Oncol* 2003; **21**: 4336-4341

26 **Piazza C**, Cocco D, De Benedetto L, Bon FD, Nicolai P, Peretti G. Role of narrow-band imaging and high-definition television in the surveillance of head and neck squamous cell cancer after chemo- and/or radiotherapy. *Eur Arch Otorhinolaryngol* 2010; **267**: 1423-1428

S- Editor Lv S **L- Editor** Webster JR **E- Editor** Zhang DN

Human Pathology (2012) 43, 356–363

ELSEVIER

Human PATHOLOGY

www.elsevier.com/locate/humpath

Original contribution

Technique for differentiating alveolar soft part sarcoma from other tumors in paraffin-embedded tissue: comparison of immunohistochemistry for TFE3 and CD147 and of reverse transcription polymerase chain reaction for ASPSCR1-TFE3 fusion transcript☆,☆☆

Kaori Tsuji DVM[a,*], Yuichi Ishikawa MD, PhD[b], Tetsuo Imamura MD[a]

[a]*Division of Surgical Pathology, Teikyo University Hospital, Tokyo 173-8606, Japan*
[b]*Division of Pathology, The Cancer Institute, Japanese Foundation for Cancer Research, Tokyo 135-8550, Japan*

Received 20 January 2011; revised 2 May 2011; accepted 4 May 2011

Keywords:
Alveolar soft part sarcoma;
Differential diagnosis;
ASPSCR1-TFE3 fusion transcript;
RT-PCR;
Immunohistochemistry

Summary The diagnosis of alveolar soft part sarcoma is commonly based on characteristic histology and distinctive periodic acid–Schiff–positive crystals; however, the characteristic crystals may not always be observed, rendering the diagnosis difficult. Three important characteristics of alveolar soft part sarcoma, the presence of ASPSCR1-TFE3 fusion transcript, nuclear immunoreactivity for TFE3, and immunoreactivity for monocarboxylate transporter 1 and CD147, have recently been reported. To identify the best marker for alveolar soft part sarcoma in formalin-fixed, paraffin-embedded tissues, we evaluated the sensitivity and specificity of the detection of the ASPSCR1-TFE3 fusion transcript along with the immunoreactivity for TFE3 and CD147 in 24 alveolar soft part sarcomas and 23 non–alveolar soft part sarcoma tumors, including 5 granular cell tumors, 5 paragangliomas, 3 clear cell sarcomas, and 10 clear cell renal cell carcinomas. The ASPSCR1-TFE3 fusion transcript was detected in 24 of 24 alveolar soft part sarcomas (7 type 1, 17 type 2), and TFE3 immunoreactivity was observed in 22 of 24 alveolar soft part sarcomas. In non–alveolar soft part sarcoma tumors, the ASPSCR1-TFE3 fusion transcript was not detected; however, the TFE3 immunoreactivity was observed in 2 of 5 granular cell tumors. CD147 immunoreactivity was demonstrated in 20 of 24 alveolar soft part sarcomas, 3 of 5 granular cell tumors, and 8 of 10 clear cell renal cell carcinomas. Our results demonstrate that the most sensitive marker of alveolar soft part sarcoma was the presence of the ASPSCR1-TFE3 fusion transcript. Thus, detection of the ASPSCR1-TFE3 fusion transcript was considered applicable for formalin-fixed, paraffin-embedded tissues with superior sensitivity as compared with TFE3 immunohistochemical staining. In alveolar soft part sarcomas with unusual locations or histology, we consider that the detection of the ASPSCR1-TFE3 fusion transcript would be the highly effective diagnostic technique.

Abbreviations: ASPS, alveolar soft part sarcoma; RCC, renal cell carcinoma; RT-PCR, reverse transcription polymerase chain reaction.

☆ Sources of funding: None.
☆☆ Disclosure of conflict of interests: None.

* Corresponding author. Division of Surgical Pathology, Teikyo University Hospital, 2-11-1 Kaga, Itabashi-ku, Tokyo 173-8606, Japan.
E-mail address: danchan@med.teikyo-u.ac.jp (K. Tsuji).

0046-8177/$ – see front matter © 2011 Elsevier Inc. All rights reserved.
doi:10.1016/j.humpath.2011.05.004

1. Introduction

Alveolar soft part sarcoma (ASPS) is a rare tumor that occurs mostly in young adults, generally in the soft tissues of the extremities. ASPS has a distinctive histology with a nest-like or organoid pattern separated by fibrovascular septa [1]. Although these features are usually diagnostic, the diagnosis of ASPS may become difficult when ASPS occurs in an unusual location, such as in the lung, stomach, retroperitoneum, and female genital tract [2]. This is, in part, because a number of more common tumors such as granular cell tumor, paraganglioma, clear cell sarcoma, and metastatic clear cell renal cell carcinoma (RCC) mimic histologic features of ASPS. The discrimination of ASPS from these tumors is critical because the management strategy differs markedly for each tumor type. Cytoplasmic crystals identified with periodic acid–Schiff staining with diastase digestion or under electron microscopy are the classical histologic features of ASPS [3]. However, such typical crystals are observed only in 22% to 80% of ASPS cases [1,4-6]. Although numerous immunohistochemical studies have been reported, a specific marker that can confirmatively diagnose ASPS has not been found thus far [2].

Recently, a tumor-specific fusion transcript for ASPS, ASPSCR1-TFE3, has been identified by the analysis of snap-frozen tumor materials, and 2 different types of fusion transcripts, that is, types 1 and 2, have been reported [7]. Subsequently, aberrant nuclear immunoreactivity for TFE3 has been reported in formalin-fixed, paraffin-embedded ASPS; however, TFE3 immunoreactivity has also been observed in 9 types of non-ASPS tumors, including high-grade myxofibrosarcoma, malignant peripheral nerve sheath tumor, granular cell tumor, chordoma, adrenal cortical carcinoma, urothelial carcinoma, distal bile duct carcinoma, pediatric RCC, and perivascular epithelioid cell neoplasm [8,9]. TFE3 immunoreactivity is highly sensitive and specific for ASPS; however, this specificity was not mutually exclusive. More recently, in a subset of perivascular epithelioid cell tumor, gene fusion involving the *TFE3* gene has been reported [10,11]. Strong immunoreactivities for monocarboxylate transporter 1 and its interacting partner CD147 have been reported for the cytoplasm of ASPS tumor cells. Unlike the positive immunoreactivity in the cytoplasmic membrane seen for many tumors, the cytoplasmic granular positivity for CD147 in the ASPS is suggested to be related to precrystalline cytoplasmic granules [12]. Based on the unique expression pattern of CD147 in ASPS, we speculated that immunoreactivity of CD147 makes it a possible diagnostic marker of ASPS, and therefore, we examined this possibility in the current study. Moreover, no comparative study has evaluated the ability of the above-mentioned 3 markers in clarifying the differential diagnosis for ASPS. Therefore, to determine the optimal method for identifying ASPS in formalin-fixed, paraffin-embedded tissues, we assessed the sensitivity and specificity of the detection of the ASPSCR1-TFE3 fusion transcript along with the immunoreactivity for TFE3 and CD147.

2. Materials and methods

2.1. Tumor specimens

Twenty-four ASPS specimens that had been embedded in paraffin were obtained from Japanese patients, of which 20 specimens were selected from the files of the authors (T.I. and Y.I.) and 4 specimens were provided by the Division of Diagnostic Pathology of the Keio University Hospital. These samples consisted of 22 primary tumors, 1 lung metastatic tumor, and 1 local recurrent tumor (Table 1). Twenty-three non-ASPS tumors, comprising 5 granular cell tumors, 5 paragangliomas, 3 clear cell sarcomas, and 10 clear cell RCCs (grades 1 and 2; 5 specimens each), were selected from the files of the Division of Surgical Pathology of the Teikyo University Hospital. Almost all the specimens were fixed in 10% to 20% formalin, and only 1 specimen (ASPS-9) was fixed in ethanol. Hematoxylin and eosin–stained slides were reviewed, and the original diagnosis was confirmed. Each 3-μm-thick serial section was used for immunohistochemical staining.

Table 1 Clinical data and results of immunohistochemical staining and RT-PCR in 24 ASPS samples

Case no.	Age (y)	Sex	Site	Source	TFE3	CD147	Fusion type
1	15	F	Thigh	P	++	++	1
2	33	M	Thigh	P	++	++	2
3	15	M	Thigh	P	++	++	1
4	61	F	Thigh	P	++	+	1
5	20	M	Thigh	P	++	+	2
6	14	M	Upper arm	P	++	+	2
7	28	M	Lower leg	P	++	++	1
8	13	F	Shoulder	P	++	+	1
9	19	M	Thigh	P	+	+	2
10	20	F	Thigh	P	++	++	2
11	53	F	Thigh	P	++	++	2
12	45	M	Lower leg	M	++	++	2
13	30	M	Thigh	P	++	−	1
14	37	M	Thigh	P	++	+	1
15	28	M	Thigh	P	++	−	2
16	24	F	Thigh	Rec	++	++	2
17	15	M	Thigh	P	++	+	2
18	29	F	Thigh	P	++	+	2
19	46	M	Back	P	−	++	2
20	44	F	Upper arm	P	++	−	2
21	13	F	Chest wall	P	++	+	2
22	19	M	Shoulder	P	−	+	2
23	16	F	Thigh	P	+	−	2
24	37	M	Thigh	P	++	+	2

Abbreviations: F, female; M, male; P, primary tumor; M, metastatic tumor; Rec, recurrent tumor.

Table 2 Primer sequences and expected product size (bp)

First PCR	Outer forward	ASPL		5′-AAAGAAGTCCAAGTCGGGCCA-3′[a]	
	Outer reverse	TFE 3	Type 1	5′-CCTTGACTACTGTACACATCAAGC-3′	132
			Type 2	5′-CATTGTAACTGGACTCCAGGC-3′	137
Nested PCR	Inner forward	ASPL		5′-AAGTCCAAGTCGGGCCAGG-3′	
	Inner reverse	TFE 3	Type 1	5′-CAGATTCCCTGACACAGGCA-3′	105
			Type 2	5′-GACTCCAGGCTGATGATCTC-3′	122
H3 histone family 3A	Forward			5′-CGAGAAATTGCTCAGGACTT-3′	
	Reverse			5′-TACACGTTTGGCATGGAT-3′	138

[a] This sequence was cited from Ladanyi et al [7].

2.2. Immunohistochemistry

Immunohistochemical staining was performed with the EnVision Detection System (Dako, Carpinteria, CA). Sections were pretreated in the microwave oven for 10 minutes in 10 mmol/L citrate acid (pH 6.0) for epitope retrieval. After cooling for 30 minutes, the sections were treated with 0.3% hydrogen peroxide to eliminate endogenous peroxidase activity. Primary antibodies, TFE3 (1:600 dilution, polyclonal, P-16, sc-5958; Santa Cruz Biotechnology, Santa Cruz, CA), and CD147 (1:100 dilution, monoclonal, clone HIM6; Research Diagnostics, Inc, Flanders, NJ) were used. The diluted antibody was applied overnight at 4°C, and the sections were developed with 3,3′-diaminobenzidine and counterstained with Mayer hematoxylin. We used a labeled polymer (Simple Stain MAX-PO [G]; Nichirei, Tokyo, Japan) for the immunohistochemical staining of TFE3 because the polymer supplied by EnVision Detection System was unavailable for goat polyclonal antibodies.

TFE3 nuclear immunoreactivity was graded on the basis of the intensity of labeling as follows: no staining (−), weak staining (+), or moderate to strong staining (++). Cytoplasmic discrete granular staining for CD147 was scored on the basis of the frequency of immunoreactive granules as follows: no staining (−), rare staining (+), or moderate to numerous staining (++). Membrane and diffuse cytoplasmic staining for CD147 were disregarded because it is known that CD147 immunoreactivity is observed in the membrane and cytoplasm of many tumors [13].

2.3. Reverse transcription polymerase chain reaction

Total RNA was extracted from paraffin-embedded tumor tissues. Five 10-μm sections from each tissue block were digested in buffer (20 mmol/L Tris-HCl, pH 8.0, 20 mmol/L EDTA, 2% sodium dodecyl sulfate) containing 10-μL of 100 mg/mL proteinase K at 55°C overnight. RNA was extracted using ISOGEN (Nippon Gene, Toyama, Japan) according to the manufacturer's instructions. The extracted RNA was then purified by phenol saturated with water. Approximately 5 μg of RNA was reverse transcribed into complement DNA using a random primer and SuperScript II (Invitrogen, San Diego, CA). The quality of RNA was assessed by amplification of H3 histone family 3A expressed ubiquitously. The amplification for the ASPSCR1-TFE3 fusion transcript was performed using Ex Taq Hot Start Version (TaKaRa, Ohtsu, Shiga, Japan); subsequently, nested polymerase chain reaction (PCR) was performed using AmpliTaq Gold (Applied Biosystems, Branchburg, NJ). Primer sequences and setting are shown in Table 2 and Fig. 1, respectively. Amplification of the first PCR consisted of denaturation at 95°C for 20 seconds, annealing at 60°C for 30 seconds, and extension at 72°C for 1 minute. After 50 cycles, 0.5 μL of the first PCR product was used as a template for the nested PCR. Touchdown PCR as nested PCR was performed, with the annealing temperature reduced by 0.5°C per cycle from 60°C to 55°C, followed by 10 further cycles at 55°C. As a positive control for the ASPSCR1-TFE3 fusion transcript, RNA extracted from 2 frozen specimens, ASPS-1 for type 1 and ASPS-2 for type 2, were used. Furthermore, a reaction mixture of reagents devoid of template complementary DNA was included in each reverse transcription (RT) PCR procedure. The PCR products were electrophoresed in 2.5% agarose gel with ethidium bromide and sequenced using an automated sequencing system (PRISM 310; Applied Biosystems, Foster City, CA).

3. Results

3.1. Immunohistochemical findings

Nuclear immunoreactivity for the TFE3 protein was observed in 22 of 24 ASPS specimens as shown in Table 1

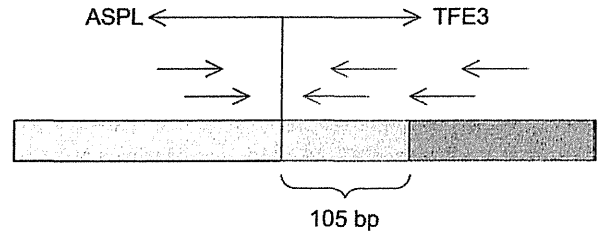

Fig. 1 Schematic diagram of the ASPSCR1-TFE3 fusion product. Sequences (105 bp long) are only found in the type 2 fusion product. Relative dimensions are approximate. Arrows indicate first (upper part) or nested (lower part) primers.

and Fig. 2. Twenty of 22 TFE3-positive ASPSs demonstrated moderate to strong (++) nuclear labeling (Fig. 2B), whereas the other 2 ASPSs demonstrated weak (+) nuclear

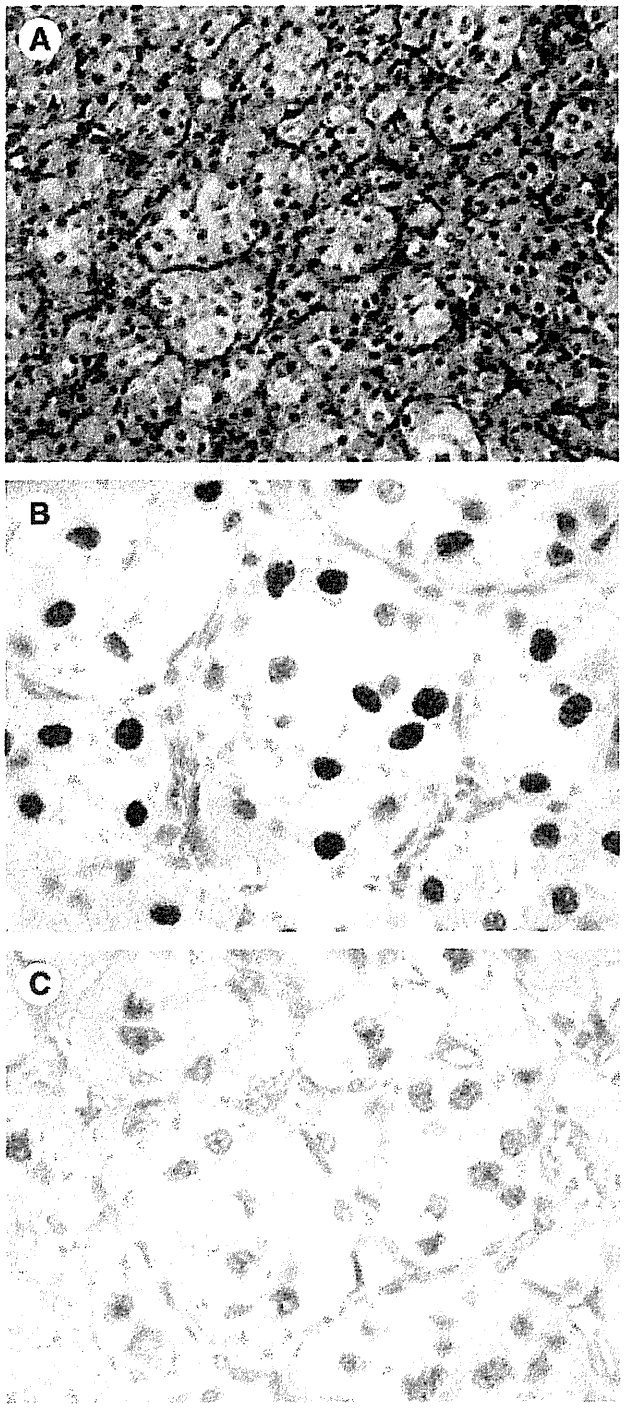

Fig. 2 TFE3 immunoreactivity in ASPS. Typical histology of ASPS showing well-defined nests of cells with abundant cytoplasm in case ASPS-6 (A; hematoxylin and eosin stain). Nuclear immunoreactivity for TFE3 showing intensive staining (++) in case ASPS-5 (B) and weak reactivity (+) in case ASPS-9 (C).

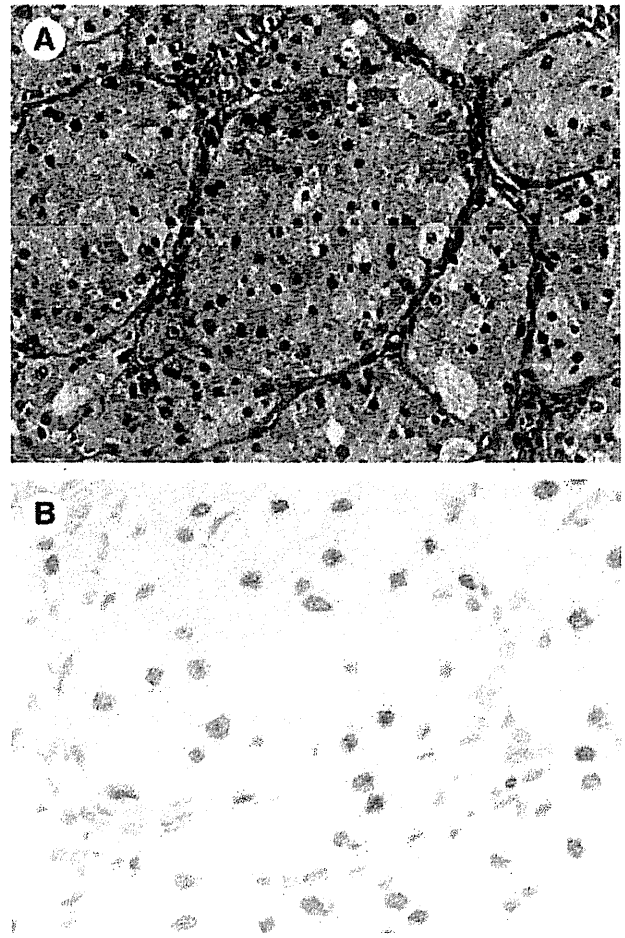

Fig. 3 TFE3 immunoreactivity in granular cell tumor. Characteristic histology of granular cell tumor showing rounded and polygonal cells with abundant granular cytoplasm (A; hematoxylin and eosin stain). Nuclear immunoreactivity for TFE3 showing moderate staining (++) (B).

labeling. One of the ASPS specimens that showed weak (+) labeling was weakly positive in only a small biopsy specimen, whereas the wide resection specimen from the same case tested negative. The other ASPS that was weakly positive (+) was the ASPS sample fixed in ethanol (Fig. 2C). In non-ASPS tumors, 2 of 5 granular cell tumors only showed nuclear immunoreactivity for TFE3 (Fig. 3). Sensitivity and specificity of TFE3 immunohistochemistry for ASPS detection were 92% and 92%, respectively. With regard to CD147 immunoreactivity, 20 of the 24 ASPSs demonstrated cytoplasmic discrete granular staining that appeared as spherical globules or polygonal inclusions (Fig. 4A, B). Similar granular inclusions for CD147 were observed in 3 of 5 granular cell tumors (Fig. 4C, D) and in 8 of 10 clear cell RCCs (Fig. 4E, F). Granular cell tumors showed small and coarse granular labeling (Fig. 4D), whereas the clear cell RCCs showed spherical globules or polygonal inclusions (Fig. 4F). ASPS and clear cell RCC grade 2 samples

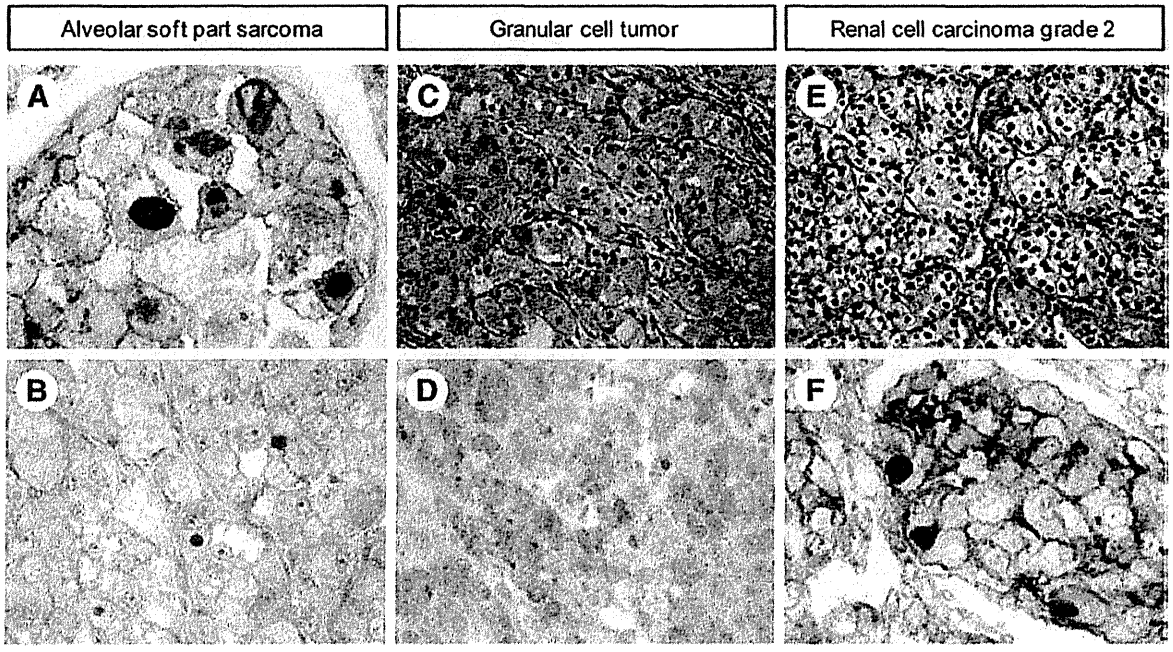

Fig. 4 Immunohistochemical staining for CD147. Cytoplasmic discrete granular staining in cases ASPS-1 (A) and ASPS-5 (B). Granular cell tumor (C; hematoxylin and eosin stain) and small and coarse granular labeling for CD147 (D). Clear cell RCC grade 2 (E; hematoxylin and eosin stain) and CD147 immunoreactivity (F). Clear cell RCC grade 2 bears a strong resemblance to ASPS.

showed a strikingly similar immunoreactive pattern. Sensitivity and specificity of CD147 immunohistochemistry for ASPS detection were 83% and 52%, respectively.

3.2. Molecular findings

In all the 24 ASPSs, the ASPSCR1-TFE3 fusion transcript was detected by RT-PCR (Fig. 5). The fusion transcripts were composed of 7 type 1 and 17 type 2 transcripts as shown in Table 1. The ASPSCR1-TFE3 fusion transcript was not detected in any of the 23 non-ASPS tumors despite sufficient amplification of the internal control H3 histone family 3A. Sensitivity and specificity of ASPSCR1-TFE3 fusion transcript for ASPS detection were 100% for both.

4. Discussion

In the present study, we have shown that the most sensitive marker of ASPS is the presence of the ASPSCR1-TFE3 fusion transcript (100% sensitivity), although immunohistochemistry for TFE3 is highly sensitive (92% sensitivity). The RT-PCR assay designed for formalin-fixed, paraffin-embedded samples can be considered the most powerful tool currently available for identifying ASPS.

Immunohistochemical staining for TFE3 is now often performed for identifying ASPS occurring in unusual locations, such as in the breast, urinary bladder, and uterine cervix [14-16], because TFE3 immunoreactivity in ASPS was first described [8]. This is reasonable because of its high sensitivity, specificity, and practicality. However, on the basis of studies investigating much wider spectra of tumors than our present study, the specificity of TFE3 immunohistochemistry is not necessarily high. In fact, 9 different types of tumors with TFE3 immunoreactivity are known [8,9]. Strong TFE3 immunoreactivity has been reported in a subset of perivascular epithelioid cell tumor and RCCs due to genetic alterations involving *TFE3* [8,10,11,17]. These results indicate that TFE3-positive findings do not always lead to a confirmed diagnosis. For the accurate diagnosis of ASPS, careful investigation would be required, including clinical findings, histologic features, identification of characteristic crystals, immunohistochemical staining for melanocytic marker (to differentiate from perivascular epithelioid cell tumor), and immunoreactivity for S-100 protein (to differentiate from granular cell tumor) [1,11].

The sensitivity of TFE3 immunohistochemistry is also problematic. In this study, 2 ASPS specimens (ASPS-19 and ASPS-22) did not show any TFE3 immunoreactivity. We believe that these negative results were false negative because the ASPSCR1-TFE3 fusion transcript was detected in these ASPSs. Because overexpression of the TFE3 protein in ASPS is probably caused by translocation including the *TFE3* gene [8], the detection of the ASPSCR1-TFE3 fusion transcript suggests that the negative TFE3 immunoreactivity result was false negative. Two other ASPS samples (ASPS-9 and ASPS-23) showed weak immunoreactivity for TFE3. This may be due to inadequate fixation or other unfavorable tissue conditions and variations in quality between different batches

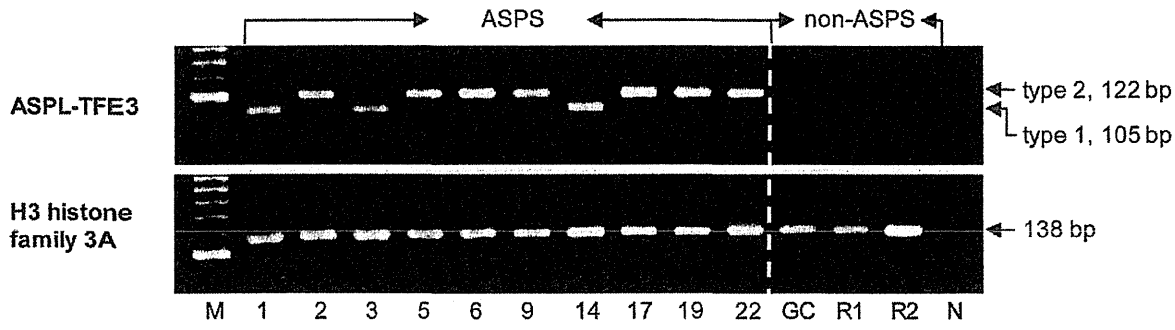

Fig. 5 RT-PCR analysis for ASPSCR1-TFE3 fusion transcripts. The upper panel shows that the fusion transcript was detected in ASPS samples, whereas non-ASPS tumors and the sample without template (N) tested negative. The lower panel shows that the internal control was detectable in all the samples. The brighter band indicates 125 bp. Abbreviations: M, 25-bp ladder marker; GC, granular cell tumor; R1 and R2, samples of clear cell RCC grade 2.

of polyclonal antibodies [17]. These findings indicate that TFE3 immunoreactivity is not entirely sensitive for ASPS; thus, a negative result cannot conclusively exclude ASPS.

Our present results demonstrated that the detection of the ASPSCR1-TFE3 fusion transcript in ASPS was more highly sensitive than TFE3 immunoreactivity. However, whether the paraffin-based RT-PCR assay is a more sensitive method than immunohistochemistry remains an unresolved question. Generally, it is known that the RNA extracted from paraffin-embedded material may have been subject to degradation; therefore, the levels of the fusion transcript may be below the detection threshold [18]. It is possible that the positive results obtained in this study were a result of the primer design, which ensured a short PCR product. We hypothesize that the shorter PCR product probably leads to higher rates of detection in RT-PCR using paraffin-embedded material. To verify the validity of this hypothesis, we compared the size of the PCR product and the detection rate of the ASPSCR1-TFE3 fusion transcript in 7 studies that analyzed the ASPSCR1-TFE3 fusion transcript in paraffin-embedded material [6,19-24]. We thus found a close correlation between the PCR product size and the detection rate of the ASPSCR1-TFE3 fusion transcript (Table 3). These findings are in accordance with the conclusions of Williams et al [21], who reported that RT-PCR techniques designed for application on paraffin-embedded material are highly sensitive and specific in detecting the ASPSCR1-TFE3 fusion transcript. An in-depth study that investigated the suitability of RNA-based analysis using various archival fixed specimens has demonstrated that the API2-MALT1 fusion transcript recognized in mucosal-associated lymphoid tissue lymphoma is amenable to RT-PCR if the fragment length is less than 150 base pairs (bp) [25]. These findings provide evidence that the PCR product size greatly affects the detection rate of the fusion transcript. In the present study, a PCR product measuring 237 bp was detected in the ASPS-9 sample that was fixed in ethanol (unpublished observations). It indicates that type 2 ASPSCR1-TFE3 fusion transcript of ASPS-9 was amplified by type 1 primer set (Fig. 1; Table 2). Ethanol fixation may be involved in low degradation or high extraction of RNA. It is known that prolonged storage of paraffin block–embedded tissues has some negative effects in RT-PCR [26]; however, 1 of our samples that was stored for 26 years, the longest storage period in the present study, was feasible for use in RT-PCR.

Furthermore, it is possible that the nested PCR performed in the present study contributed to the high detection rate of the ASPSCR1-TFE3 fusion transcript, because the increased

Table 3 Size of PCR product and detection rate of ASPSCR1-TFE3 fusion transcript

Product size (bp)			Total cases	Detected cases	Detection rate (%)	References
	Type 1	Type 2				
	116	127	6	6	100	19
	116	128	5	5	100	20
	120	130	1	1	100	6
	120	130	13	13	100	21
	126	130	1	1	100	22
First PCR	132	137	24	24	100	Present study
Nested PCR	105	122				
First PCR	190	310	16	11	69	23
Nested PCR	138	243				
	195	300	33	13	39	24

cycle number for nested PCR probably promoted an amplification of the ASPSCR1-TFE3 fusion transcript from the degraded RNA. The nested PCR in this study was originally intended to exclude certain unexpected bands recognized in non-ASPS tumors. It was highly effective for obtaining specific amplified products and, in addition, probably promoted the amplification of the fusion transcript. However, performance of nested PCR, which is an additional procedure, may increase the risk of contamination. Although a band of the correct size is obtained in the first PCR analysis in the case of many ASPSs, nested PCR can be a valuable technique in some cases of ASPS. To ensure that correct-sized bands of ASPSCR1-TFE3 fusion transcript are obtained in the first PCR, it is important to prepare some tubes with progressively increasing quantities of the template in each case. Decrease of the procedure for detection of fusion transcript will lead to a decrease in risk of contamination.

Finally, all our 24 ASPS samples contained type 1 or type 2 fusion variants. If an unknown variant were present in the ASPS samples, such a case would have presented as a negative result by this RT-PCR analysis. Although the distinction between type 1 and type 2 fusion variants was not the aim of this study, our result showed that the frequency of detection of the type 2 variant was twice that of the type 1 variant; this finding does not agree with the comparisons described in previous reports [6,7,19-24]. In Japanese patients with ASPS, the type 2 variant may be the predominant form rather than type 1.

CD147 has been originally identified as a tumor surface protein capable of inducing matrix metalloproteinase expression in fibroblasts [27]. Overexpression of CD147 has been noted in a number of tumors and is known to contribute to tumor invasion and metastasis [13,27]. In the present study, CD147 immunoreactivity was observed not only in ASPS but also in granular cell tumor and clear cell RCC as cytoplasmic granules; furthermore, the cell membranes of 23 of the 24 ASPSs showed strong immunoreactivity for CD147 (unpublished observations). This finding leads us to conjecture that the expression of CD147 may be related to the early metastasis of ASPS, which presents frequently. The expression of CD147 in ASPS would be valuable as an anticancer target rather than as merely a diagnostic marker.

In the present study, we have demonstrated that the detection of the ASPSCR1-TFE3 fusion transcript is the most sensitive marker for identifying ASPS and is applicable to paraffin-embedded tissues with accuracy superior to immunohistochemical staining for TFE3. Fortunately, we were able to use the tissue blocks with good condition and also able to obtain sufficient RNA for examination of ASPSCR1-TFE3 fusion transcript. Obtaining adequate RNA is probably the most important in detection of the fusion transcript using paraffin-embedded samples. In case of a small biopsy sample or a consultation case in which unstained slides were offered, sufficient RNA may not be extracted, and RT-PCR analysis may fail. In such a case, fluorescence in situ hybridization (FISH) assay is an effective way to identify the presence of a *TFE3* gene fusion in paraffin-embedded material [17,20]. The results obtained using the RT-PCR method were unexpectedly high in terms of specificity and sensitivity, making it feasible for assays using archival materials from the hospital pathology department and which is expected to be especially useful for studies involving large numbers of cases of more or less rare diseases as well as for the differential diagnosis of tumors with tumor-specific fusion transcripts.

Acknowledgment

The authors thank Dr. Makio Mukai of the Keio University Hospital for providing paraffin-embedded ASPS materials and the relevant clinical information.

References

[1] Weiss SW, Goldblum JR. Malignant soft tissue tumors of uncertain type. Enzinger and Weiss's soft tissue tumors. 5th ed. Philadelphia, PA: Elsevier Mosby; 2008. p. 1161-220.
[2] Ordonez NG. Alveolar soft part sarcoma: a review and update. Adv Anat Pathol 1999;6:125-39.
[3] Shipkey FH, Lieberman PH, Foote FW, et al. Ultrastructure of alveolar soft part sarcoma. Cancer 1964;17:821-30.
[4] Lieberman PH, Brennan MF, Kimmel M, et al. Alveolar soft-part sarcoma. A clinicopathologic study of half a century. Cancer 1989;63: 1-13.
[5] Tucker JA. Crystal-deficient alveolar soft part sarcoma. Ultrastruct Pathol 1993;17:279-86.
[6] Kacerovska D, Michal M, Nemcova J, et al. Crystal-deficient alveolar soft-part sarcoma with cutaneous involvement: a case report. Am J Dermatopathol 2009;31:272-7.
[7] Ladanyi M, Lui MY, Antonescu CR, et al. The der(17)t(X;17)(p11; q25) of human alveolar soft part sarcoma fuses the TFE3 transcription factor gene to ASPL, a novel gene at 17q25. Oncogene 2001;20:48-57.
[8] Argani P, Lal P, Hutchinson B, et al. Aberrant nuclear immunoreactivity for TFE3 in neoplasms with *TFE3* gene fusions: a sensitive and specific immunohistochemical assay. Am J Surg Pathol 2003;27: 750-61.
[9] Folpe AL, Mentzel T, Lehr HA, et al. Perivascular epithelioid cell neoplasms of soft tissue and gynecologic origin: a clinicopathologic study of 26 cases and review of the literature. Am J Surg Pathol 2005;29:1558-75.
[10] Tanaka M, Kato K, Gomi K, et al. Perivascular epithelioid cell tumor with *SFPQ/PSF-TFE3* gene fusion in a patient with advanced neuroblastoma. Am J Surg Pathol 2009;33:1416-20.
[11] Argani P, Aulmann S, Illei PB, et al. A distinctive subset of PEComas harbors *TFE3* gene fusions. Am J Surg Pathol 2010;34:1395-406.
[12] Ladanyi M, Antonescu CR, Drobnjak M, et al. The precrystalline cytoplasmic granules of alveolar soft part sarcoma contain monocarboxylate transporter 1 and CD147. Am J Pathol 2002;160:1215-21.
[13] Riethdorf S, Reimers N, Assmann V, et al. High incidence of EMMPRIN expression in human tumors. Int J Cancer 2006;119: 1800-10.
[14] Wu J, Brinker DA, Haas M, et al. Primary alveolar soft part sarcoma (ASPS) of the breast: report of a deceptive case with xanthomatous features confirmed by TFE3 immunohistochemistry and electron microscopy. Int J Surg Pathol 2005;13:81-5.
[15] Amin MB, Patel RM, Oliveira P, et al. Alveolar soft-part sarcoma of the urinary bladder with urethral recurrence: a unique case with

emphasis on differential diagnoses and diagnostic utility of an immunohistochemical panel including TFE3. Am J Surg Pathol 2006;30:1322-5.
[16] Roma AA, Yang B, Senior ME, et al. TFE3 immunoreactivity in alveolar soft part sarcoma of the uterine cervix: case report. Int J Gynecol Pathol 2005;24:131-5.
[17] Zhong M, De Angelo P, Osborne L, et al. Dual-color, break-apart FISH assay on paraffin-embedded tissues as an adjunct to diagnosis of Xp11 translocation renal cell carcinoma and alveolar soft part sarcoma. Am J Surg Pathol 2010;34:757-66.
[18] Cataldo KA, Jalal SM, Law ME, et al. Detection of t(2;5) in anaplastic large cell lymphoma: comparison of immunohistochemical studies, FISH, and RT-PCR in paraffin-embedded tissue. Am J Surg Pathol 1999;23:1386-92.
[19] Jun HJ, Lee J, Lim do H, et al. Expression of MET in alveolar soft part sarcoma. Med Oncol 2010;27:459-65.
[20] Aulmann S, Longerich T, Schirmacher P, et al. Detection of the *ASPSCR1-TFE3* gene fusion in paraffin-embedded alveolar soft part sarcomas. Histopathology 2007;50:881-6.
[21] Williams A, Bartle G, Kindblom LG, et al. Identification of the ASPL/TFE3 fusion transcript and immunohistochemical detection of TFE3 in formalin-fixed paraffin-embedded tissue: their role in the diagnosis of alveolar soft part sarcoma (ASPS). Poster Presentation at: USCAP; March 1–7, 2008.
[22] Bodi I, Gonzalez D, Epaliyange P, et al. Meningeal alveolar soft part sarcoma confirmed by characteristic *ASPCR1-TFE3 fusion*. Neuropathology 2009;29:460-5.
[23] Pang LJ, Chang B, Zou H, et al. Alveolar soft part sarcoma: a biomarker diagnostic strategy using TFE3 immunoassay and ASPL-TFE3 fusion transcripts in paraffin-embedded tumor tissues. Diagn Mol Pathol 2008;17:245-52.
[24] Lazar AJ, Das P, Tuvin D, et al. Angiogenesis-promoting gene patterns in alveolar soft part sarcoma. Clin Cancer Res 2007;13:7314-21.
[25] Liu H, Huang X, Zhang Y, et al. Archival fixed histologic and cytologic specimens including stained and unstained materials are amenable to RT-PCR. Diagn Mol Pathol 2002;11:222-7.
[26] Mizuno T, Nagamura H, Iwamoto KS, et al. RNA from decades-old archival tissue blocks for retrospective studies. Diagn Mol Pathol 1998;7:202-8.
[27] Iacono KT, Brown AL, Greene MI, et al. CD147 immunoglobulin superfamily receptor function and role in pathology. Exp Mol Pathol 2007;83:283-95.

Cancer Science
The official journal of the Japanese Cancer Association JCA

Prevalence of human papillomavirus in mobile tongue cancer with particular reference to young patients

Masayuki Kabeya,[1,2] Reiko Furuta,[1] Kazuyoshi Kawabata,[3] Sugata Takahashi[2] and Yuichi Ishikawa[1,4]

[1]Division of Pathology, The Cancer Institute, Japanese Foundation for Cancer Research, Tokyo; [2]Department of Otolaryngology, Niigata University Faculty of Medicine, Niigata; [3]Department of Head and Neck Oncology, The Cancer Institute Hospital, Japanese Foundation for Cancer Research, Tokyo, Japan

(Received July 7, 2011/Revised October 6, 2011/Accepted October 28, 2011/Accepted manuscript online November 9, 2011/Article first published online December 15, 2011)

The carcinogenetic role of human papillomavirus (HPV) in mobile tongue cancer remains unclear because of conflicting results reported in the literature. This disparity is likely to be due to variations in the samples and methods used. Furthermore, despite a tendency for increased prevalence of mobile tongue cancer in young adults, only a few reports specifically in young patients have been published. In the present study on 32 patients, including six in their 20s, we genotyped the prevalence of HPV using a highly sensitive detection tool in fresh-frozen samples from surgical specimens and a novel detection device with electrochemical DNA chip and loop-mediated isothermal amplification. In addition, we confirmed HPV prevalence by *in situ* hybridization and immunohistochemistry for the $p16^{INK4a}$ protein, regarded as a biomarker of HPV-associated cancers. The frequency of 13 genotypes of high-risk HPV was 0/32 (0%), which was further confirmed by *in situ* hybridization. Overexpression of $p16^{INK4a}$ protein was observed in six of the 32 patients (19%), with four (67%) also overexpressing p53. Because there is usually a lack of p53 overexpression in HPV-associated cancer, it is unlikely that $p16^{INK4a}$ protein overexpression is correlated with HPV infection. Consequently, it is unlikely that HPV infection plays an important role in mobile tongue carcinogenesis, in particular in young adults. In addition, our data suggest that the overexpression of $p16^{INK4a}$ protein is not an appropriate biomarker for HPV association in mobile tongue carcinogenesis. (*Cancer Sci* 2012; 103: 161–168)

Human papillomavirus (HPV) is a small DNA virus and more than 130 different types of HPV have been identified based on DNA sequence variations.[1,2] Human papillomavirus is divided into low-risk and high-risk types, depending on the carcinogenic power.[3] It has been conclusively established that more than 99% of uterine cervical cancers are associated with HPV infection.[2,4] Because HPV-associated cancers may be prevented with vaccination,[5–7] it is important to determine whether cancer of extracervical organs is associated with HPV infection.[8,9] Among the head and neck cancers, oropharyngeal cancer, particularly tonsillar cancer, and basal tongue cancer are known to be strongly associated with HPV infection.[3] However, the role of HPV in mobile tongue cancer (MTC) remains unclear because of the disparity of results published so far, which have reported HPV infection rates ranging from 0% to 100%.[10–20] This disparity may be due to differences in the types of samples used and the methods of detection. A recent study has reported an increasing incidence of MTC among young adults.[21] Thus far, alcohol consumption and heavy cigarette smoking have been suggested as causal factors for MTC.[11,13] However, it is difficult to explain the high incidence of MTC in young adults simply as a result of accumulated exposure to alcohol and smoking.[11,21,22] To date, there have been only a few reports on relationship between MTC (as well as tonsillar cancers) and HPV in young patients.[23]

The primary aim of the present study was to determine the prevalence of HPV in MTC using a comprehensive assay series. To that end, we screened rapidly frozen surgical specimens that were subsequently assayed with electrochemical DNA chips (EC chips) and the loop-mediated isothermal amplification (LAMP) method. We confirmed HPV infection using other methodologies, such as *in situ* hybridization (ISH) and immunohistochemistry (IHC) to investigate the overexpression of $p16^{INK4a}$ protein.[24] The secondary aim of the study was to elucidate whether overexpression of $p16^{INK4a}$ protein is an appropriate marker HPV infection.

Materials and Methods

Patients. Thirty-two patients presenting with untreated MTC who subsequently underwent surgical resection at the Cancer Institute Hospital, Japanese Foundation for Cancer Research (JFCR), between January 2006 and December 2009 were enrolled in the study. All samples were dissected from a main viable part of each tumor and snap-frozen in liquid nitrogen, typically within 20 min of removal, and stored at −80°C until processing. Histological diagnosis and grading were performed using sections stained with H&E, made from formalin-fixed and paraffin-embedded tissues, based on the World Health Organization (WHO) classification.[25] Each tumor was staged according to the Cancer Staging Manual of American Joint Committee on Cancer TNM classification.[26] All samples were collected from patients who had provided informed consent, and the study was approved by the Institutional Review Board of the JFCR.

Histological sub-classification. As described previously,[27,28] squamous cell carcinoma (SCC) of MTC was divided into three groups based on histological features: (i) non-keratinizing (NK) SCC; (ii) keratinizing (K) SCC; and (iii) hybrid SCC. This division is thought to be particularly useful for the analysis of HPV-related SCC because HPV-related tonsillar cancer may derive from the cryptal epithelium, having a more basaloid nature, whereas non-related tonsillar cancer may originate from the surface epithelium.[29,30] Briefly, NK SCC is defined as forming sheets, nests, or trabeculae with pushing borders and forms comedo-type necrosis. Tumors have ovoid to spindled hyperchromatic cells that lack prominent nucleoli and have indistinct cell borders. In the present study, K SCC was defined as that composed entirely of mature squamous cells with keratinization and intercellular bridges without areas exhibiting NK SCC morphology. Hybrid SCC was defined as SCC having definitive areas with NK SCC morphology but exhibiting squamous maturation

[4]To whom correspondence should be addressed. E-mail: ishikawa@jfcr.or.jp

doi: 10.1111/j.1349-7006.2011.02149.x

in >10% of the tumor. We also used conventional differentiation grading of SCC.

Immunohistochemistry. Formalin-fixed, paraffin-embedded (FFPE) tumor-rich blocks were prepared for p53 and $p16^{INK4a}$ IHC. After deparaffinization, the sections were submerged in either sodium citrate buffer or Tris–EDTA buffer for heat-induced epitope retrieval at 97°C for 40 min. The immunostaining was performed using the EnVision + dextran polymer kit (Dako, Tokyo, Japan) and the CINtec histology kit (MTM Laboratories, Heidelberg, Germany) using a Dako Autostainer (Dako, Glostrup, Denmark). A positive control consisting of an invasive cervical cancer was included. Results were evaluated by one pathologist (YI). "Positive cells" were defined as those exhibiting strong nuclear and cytoplasmic staining for $p16^{INK4a}$ and strong nuclear staining for p53, and we classified tumors in terms of the percentage positive cell as follows: 0, negative; 1+, 1–25% positive cells; 2+, 26–50% positive cells; 3+, 51–75% positive cells; and 4+, >75% positive cells.

***In situ* hybridization.** Additional sections were prepared and deparaffinized for HPV DNA detection using ISH. The ISH was performed using a wide-spectrum HPV biotinylated DNA probe (Dako) for common HPV types and the GenPoint amplification system (Dako) according to the manufacturer's instructions. This wide-spectrum probe targets the genomic DNA of HPV types 6, 11, 16, 18, 31, 33, 35, 39, 45, 51, and 52. In each series, a positive control sample, consisting of a tonsillar cancer already identified as HPV positive, was included. Punctate nuclear staining (brown nuclear dots) was considered as positive.

Detection of HPV DNA. Fresh-frozen blocks were added to individual tubes in addition to 200 μL virus standard buffer (comprising 10 mL of 5 M NaCl, 10 mL of 1 M Tris–HCl (pH 7.5), 5 mL of 0.1 M EDTA-2Na (pH 7.5), and 975 mL milliQ water). Each sample was homogenized, followed by the addition of 700 μL virus standard buffer, 100 μL of 10% SDS, and 25 μL of 25 mg/mL proteinase K solution. Samples were incubated overnight at 37°C. After digestion, DNA purification was performed by phenol–chloroform extraction and ethanol precipitation. The quantity and quality of the DNA were assessed by spectrophotometry and electrophoresis on a 1% agarose gel. The DNA solutions were stored at 4°C.

Human papillomavirus detection and genotyping were performed using an HPV DNA genotyping system. The DNA extracted from each sample was incubated at 95°C for 5 min and then cooled immediately on ice. A 1-μL aliquot of the DNA was added to each of the six LAMP tubes, containing 24 μL LAMP reagent and specific primers for the different types of HPV. The tubes were incubated at 65°C for 90 min, then at 80°C for 5 min, and the cooled immediately on ice. A 10-μL aliquot of the amplified products from each tube was mixed with 6 μL hybridization buffer (saline citrate solution), and 50 μL mixed LAMP product was applied to an EC chip, which uses novel current detection technology (CLINICHIP HPV; Sekisui-medical, Tokyo, Japan). The EC chip was placed in Genelyzer GLH-2C601 (Toshiba Hokuto Electronics, Asahikawa, Japan), which is an instrument designed to measure electrochemical signals from the EC chip. A positive control was included in each series, consisting of an invasive cervical cancer. The results were evaluated automatically. The principle of measurement was as follows. Thirteen DNA types (type 16, 18, 31, 33, 35, 39, 45, 51, 52, 56, 58, 59, and 68) of high-risk HPV were amplified using the LAMP method with 13 primers that amplify HPV DNA in a type-specific manner. This HPV DNA genotyping assay targets the L1 open reading frames, conserved among most of the HPV genomes. The DNA probes for the target genes are fixed on the electrodes of the EC chip. When HPV DNA extracted from samples is amplified and introduced to the EC chip, it reacts and binds only with the probe with the complementary sequence. Subsequently, when an intercalator (i.e. labeling reagent for the double-strand structure) is added, it only combines with the DNA that has reacted and current flows only between the bound intercalator and the EC chip electrode. The sequence of the sample DNA is determined by detecting this current. The criteria used to evaluate the samples were as follows. Positive samples were scored where the current level of the test specimen was higher than that of the average for the negative control by ≥10 nA. Negative samples were scored where the difference in current levels between the test specimen and the average of the negative control was within 10 nA. Invalid samples were scored when the average current level of the negative control was >45 nA. All genotypes were detected at a 100% positive at HPV DNA 250 copies per 1 μL. The HPV genotypes determined by this HPV DNA genotyping system for 244 test clinical samples were compared with direct PCR sequencing using specific primers for 13 genotypes. The concordance rate for HPV genotyping was 95.5% (233/244).

Statistical analysis. Statistical analyses for a correlation between age groups, younger (20–39 years) and older patients (40–90 years), or immunoreactivity and the clinical outcome were performed using Fisher's exact test. Differences in disease-free survival and overall survival between younger (20–39 years) and older patients (40–90 years) were evaluated using the Kaplan–Meier method, starting from the date of surgery. Survival curves was compared using the log-rank test. $P < 0.05$ was considered significant.

Results

Table 1 lists the characteristics of the 32 patients in the present study. Twenty-nine patients (91%) were male and three (9%) were female. The age of the patients ranged between 21 and 90 years, with a median age 55 years. Ten patients (31%), including six who were in their 20s, were younger than 40 years. The mean follow-up time was 26.1 months, with a maximum of 53 months. One of 32 patients was diagnosed histologically as having spindle cell carcinoma, whereas the others were all diagnosed with standard SCC. The patient with spindle cell carcinoma was a 55-year-old male smoker who also had the heaviest alcohol consumption per day among the 32 patients. The spindle cell carcinoma recurred in 10 months and the patient died 23 months after surgery. Most patients had well-differentiated tumors, but three had moderately (26-, 44-, and 76-year-old men) and two had poorly (31- and 38-year-old men) differentiated tumors. Although the three patients with moderately differentiated tumors had no recurrence, tumors in the two patients with poorly differentiated tumors recurred: one

Table 1. Patient and tumor characteristics

Sex (*n*)	
Male/female	29/3
Age (years)	
Median (range)	55 (21–90)
Tumor histology (*n*)	
SCC/spindle cell carcinoma	31/1
Histological grade of SCC (*n*)	
Well/moderately/poorly differentiated	26/3/2
Pathological stage* (*n*)	
I+II/III+IV	8/22
Alcohol consumption (*n*)	
Yes/no/incidental	11/10/11
Cigarette exposure (*n*)	
Yes/no/former smoker	12/12/8

*Excluding two patients in whom regional lymph nodes could not be assessed. Alcohol consumption categorized as "yes" indicated daily, whereas that categorized as "incidental" indicated social drinkers. SCC, squamous cell carcinoma.

doi: 10.1111/j.1349-7006.2011.02149.x

Table 2. Clinicopathologic features, results of immunohistochemistry ($p16^{INK4a}$and p53 status), ISH, human papillomavirus DNA detection, and clinical outcome

Patient no.	Age (years)	Sex	pTN	Histologic features*	$p16^{INK4A}$ expression†	p53 expression†	ISH	GS‡	Outcome
1	21	M	pT2N2b	Hybrid SCC	4+	4+	–	–	Death
2	25	M	pT1N0	K SCC	–	4+	–	–	Death
3	26	M	pT3N2b	K SCC	3+	4+	–	–	No recurrence
4	27	M	pT3N1	K SCC	–	3+	–	–	Death
5	28	M	pT2N0	K SCC	–	3+	–	–	Death
6	28	M	pT4aN2b	K SCC	–	4+	–	–	No recurrence
7	31	M	pT2N2b	Hybrid SCC	–	–	–	–	Death
8	33	M	pT4aN2b	Hybrid SCC	–	4+	–	–	Death
9	35	M	pT2N2b	Hybrid SCC	–	4+	–	–	Death
10	38	M	pT1N0	Hybrid SCC	–	–	–	–	Recurrence, alive
11	44	M	pT4aN0	Hybrid SCC	–	–	–	–	No recurrence
12	47	M	pT2N2	K SCC	–	–	–	–	No recurrence
13	48	M	pT2N0	K SCC	2+	1+	–	–	No recurrence
14	49	F	pT3N1	Hybrid SCC	–	4+	–	–	No recurrence
15	51	M	pT3N0	K SCC	–	–	–	–	No recurrence
16	55	M	pT3N0	Spindle CC	–	4+	–	–	Death
17	55	M	pT2N0	K SCC	–	–	–	–	No recurrence
18	57	M	pT1N0	K SCC	–	–	–	–	No recurrence
19	59	M	pT2N0	K SCC	1+	1+	–	–	No recurrence
20	60	F	pT3N2c	Hybrid SCC	–	3+	–	–	Death
21	64	M	pT2N2b	K SCC	–	3+	–	–	DOD
22	68	M	pT2N2b	K SCC	–	2+	–	–	DOD
23	69	M	pT3N0	K SCC	–	–	–	–	No recurrence
24	71	M	pT2NX	K SCC	4+	–	–	–	No recurrence
25	72	M	pT2N1	K SCC	1+	–	–	–	No recurrence
26	76	M	pT2N0	Hybrid SCC	–	–	–	–	No recurrence
27	77	M	pT4aN2b	Hybrid SCC	–	4+	–	–	Death
28	78	M	pT3N2b	K SCC	–	3+	–	–	Death
29	79	M	pT2N2b	K SCC	–	1+	–	–	Death
30	80	F	pT3N2b	K SCC	–	4+	–	–	Death
31	85	M	pT3N2b	K SCC	–	–	–	–	Death
32	90	M	pT2NX	K SCC	–	–	–	–	Death

*Tumors were classified into three types histologically: (i) keratinizing squamous cell carcinoma (K SCC); (ii) non-keratinizing squamous cell carcinoma (NK SCC); and (iii) mainly NK SCC but with areas of squamous maturation (Hybrid SCC). †The percentage of positive-stained cells were scored as follows: 0, negative; 1+, 1–25% positive cells; 2+, 26–50% positive cells; 3+, 51–75% positive cells; and 4+, >75% positive cells. Note, $p16^{INK4A}$-positive cells were those in which both the nucleus and cytoplasm were stained, whereas p53-positive cells exhibited nuclear staining only. ‡The genotyping system (GS) used in the present study is a novel tool to detect 13 types of high-risk human papillomavirus (HPV) strains using electrochemical technology and loop-mediated isothermal amplification (LAMP). DOD; death from other disease. IHC; *in situ* hybridization, Spindle CC; spindle cell carcinoma.

within 7 months, with the patient dying 30 months after surgery, and the other within 8 months. This second patient is still alive 40 months after surgery, although at a terminal stage.

Regarding pathologic stages, eight patients (27%) were in early Stages I/II, 22 (73%) were in advanced Stages III/IV, and two were unstaged because their lymph nodes were not examined. Of the eight patients in early Stages I/II, three (38%) were younger and five (62%) were older than 40 years of age. Two (67%) of the three younger patients in early Stages I/II had local recurrence, whereas none (0%) of the five older patients had any recurrence ($P = 0.107$). Of the 22 patients with advanced Stages III/IV, seven (32%) were younger and 15 (68%) were older than 40 years of age. The percentage of patients with an unfavorable outcome was 72% (5/7) in the younger age group and 54% (7/13) in the older age group ($P = 0.392$). The remaining two patients in whom staging was not performed died from other diseases. Therefore, there were no significant differences in the prognosis between younger (<40 years) and older (>40 years) patients.

Of the 32 patients, 12 (38%) were daily smokers, eight (24%) were past smokers, and 12 (38%) were life-time non-smokers. The mean cumulative smoking cigarette volume was 31.6 pack-years for the 12 daily smokers and 11.9 for the eight past-smokers. Only 11 of the 32 patients (34%) in the present study were drinkers. In addition, seven of the 32 patients (22%) were neither smokers nor consumers of alcohol and one of these seven was in his 20s.

Table 2 gives the clinicopathological features and results of IHC ($p16^{INK4a}$ and p53), ISH, HPV DNA detection and genotyping analyses. The 32 tumors were classified histologically as one spindle cell carcinoma and 31 SCCs. Of the 31 SCCs, 21 (68%) were classified as K SCC (Fig. 1a), none (0%) was found to be an NK SCC, and 10 (32%) were determined to be hybrid SCC (Fig. 1b). Overexpression of $p16^{INK4a}$ was noted in six of 32 patients (19%; Fig. 2a). The grading of the $p16^{INK4a}$-positive tumors was as follows: two were 1+, one was 2+, one was 3+, and two were 4+. Two of three tumors (67%) with strong reactivity (3+ or 4+) were in patients who were aged in their 20s. Only one of six patients (17%) with overexpression of $p16^{INK4a}$ experienced local recurrence and died, whereas 14 of 26 patients (54%) without $p16^{INK4a}$ overexpression died, indicating a prognostic value of $p16^{INK4a}$, although the difference failed to reach statistical significance in the current sample set ($P = 0.116$). Overexpression of p53 was noted in 19 of 32 tumors (59%;

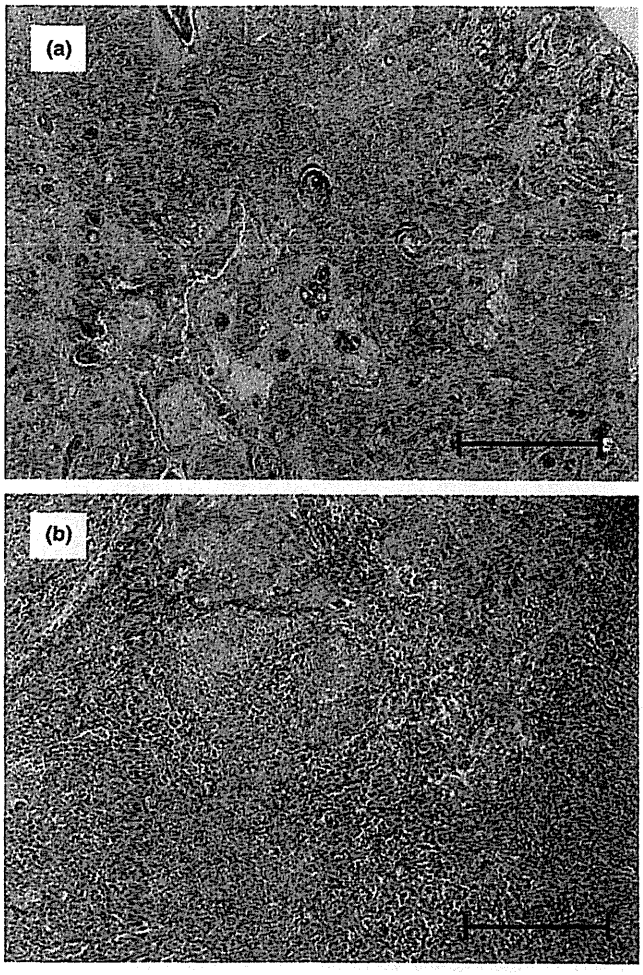

Fig. 1. Histological features (H&E stain). (a) Squamous cell carcinoma (SCC) composed entirely of keratinizing malignant cells and (b) SCC composed mainly of non-keratinizing malignant cells but also exhibiting partly formed squamous maturation (hybrid SCC). Scale lines, 1.00 mm (a); 400 μm (b).

Fig. 2b). Specifically, 13 tumors were not stained, four were weakly stained (three 1+ tumors and one in 2+ tumor), and 15 were strongly stained (five 3+ tumors and ten 4+ tumors). Eight of 10 patients (80%) who were <40 years of age were found to overexpress p53. Eleven of the 15 patients (73%) with strong p53 overexpression died of MTC, one from another disease; in contrast of the 17 patients with no or only weak p53 expression, only four (24%) died of MTC, one from another disease. All other patients survived. Therefore, patients with strong p53 overexpression had a significantly less favorable prognosis than those with weak or no p53 expression ($P < 0.01$). With ISH using the wide-spectrum probes against carcinogenic HPV DNA, none of the samples in our series showed the punctate pattern, correlated with viral DNA integration (Fig. 2c). Consequently, although we used two carcinogenic HPV DNA detection methods (i.e. ISH and the novel HPV DNA genotyping system) and they worked well for a positive control case with tonsillar and cervical cancer (Figs 2d and 3b), all samples of MTC were negative (Figs 2c and 3a).

The 3-year disease-free and overall survival rates were 48% and 50%, respectively. The prognosis for younger patients (20–39 years) was less unfavorable than that for older (40–90 years) patients in terms of both disease-free and overall survival. A significant difference was found between these two age groups in terms of disease-free survival ($P = 0.027$), but not for overall survival ($P = 0.102$; Fig. 4).

Discussion

It is important to determine whether extracervical cancers are associated with HPV because these cancers may be preventable by HPV vaccination. Of the extracervical sites, tumors in the oral cavity, oropharyx, esophagus, penis and anus are possibly associated with HPV because of its route of infection[31–33] and, indeed, tumors in these sites exhibit morphological similarities.[16,30] Of the head and neck cancers, oropharyngeal cancer is related to HPV, as is tonsillar cancer in particular, with detection rates of HPV16, HPV18, and/or HPV33 reported in the range of 21–100%.[19,34–36] Interestingly, HPV-positive tumors have been reported to respond better to chemoradiotherapy than HPV-negative tumors and survival is longer in patients with HPV-positive tumors than those with -negative tumors.[23,37–41] Although the importance of carcinogenic HPV infection is well recognized for diagnostic and therapeutic strategies in tonsillar cancer, the prevalence of HPV in MTC (adjacent to tonsillar cancer) remains uncertain. In the present study, we evaluated the prevalence of carcinogenic HPV infection and investigated the correlation between $p16^{INK4a}$ protein expression and HPV. We found that there was no evidence of carcinogenic HPV infection in MTC and that the $p16^{INK4a}$ protein was not an appropriate marker of HPV infection.

Although the possibility that HPV is relevant to MTC has been suggested, there are no reliable prevalence data supporting this assertion. This may be due mainly to the diverse target groups or methodologies used by different studies. In fact, some previous studies have classified MTC as an oral cancers,[14,42] which is too broad a classification to allow causal agents to be specified. Furthermore, different studies have used different experimental procedures: ISH, Southern blot hybridization, IHC and PCR have been used for detection; brush, biopsy, and surgery have been used for sampling; and fresh-frozen or FFPE tissue blocks have been used for storage.[43,44] Fresh-frozen materials seem to provide higher detection rates than FFPE samples, probably because of target DNA degeneration following formalin fixation; furthermore, PCR methods appear to be more sensitive than others.[45] Using FFPE samples may result in the possible contamination of carcinogenic HPV DNA at the time of sectioning.[13] Therefore, in the present study, we chose to use fresh-frozen materials from surgical specimens to avoid both DNA degeneration and contamination. In addition, the LAMP method used in the present study is reportedly equivalent to, or even more sensitive than, PCR.[46,47] We also used ISH for additional confirmation of HPV DNA. Thus, we tried to achieve higher sensitivity and higher accuracy than in previous studies.

In addition to differences in the methodologies used in previous studies, the wide range in the prevalence of HPV reported in different studies may be ascribed to variations in the nature of HPV-associated cancers. For example, a geographic heterogeneity of HPV-associated cancers has been reported. In India and Southeast Asia, oral cancer is a predominant malignancy, accounting for up to 50% of all cancers.[10] Similarly, HPV prevalence in oropharyngeal cancer is significantly higher in North America and Asia than in Europe.[8] Another factor that may impact on the apparent prevalence of HPV is the time period/s examined. For example, Okinawa, a subtropical island in south-west Japan, the prevalence of HPV in SCC of the lung we found to decrease significantly over a relatively short period of time, from 68% in 1995, to 35% in 1996, 23% in 1997, and 24% in 1998.[48] In the present study, all patients examined were from mainland Japan, a region with a lower prevalence of HPV

doi: 10.1111/j.1349-7006.2011.02149.x

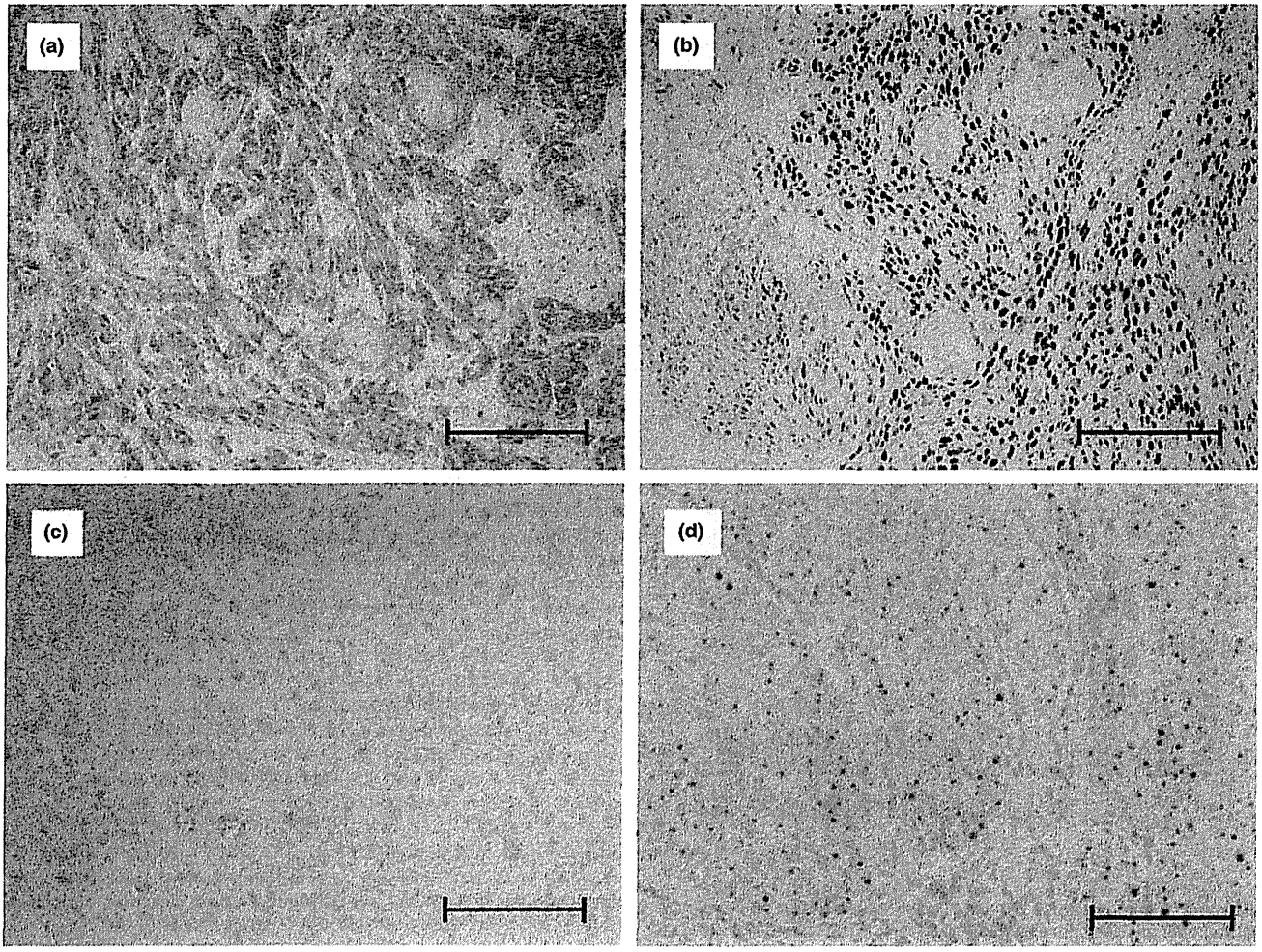

Fig. 2. (a–c) Immunohistochemical staining for $p16^{INK4A}$ (a) and p53 (b), and *in situ* hybridization (ISH) findings (c) for Patient 1 (see Table 2). (d) Tonsillar cancer positive control for ISH (brown indicates nuclear staining). (a) Strong nuclear and cytoplasmic staining was seen for $p16^{INK4A}$ (i.e. >75% positive cells) and (b) strong nuclear staining was seen for p53 (also >75% positive cells). (c) The tumor was negative by ISH. Scale lines, 200 μm (a,b); 100 μm (c,d).

infection than Okinawa. Based on the findings of the previous studies discussed above, our results of no HPV infection in MTC may be explained, in part, by the facts that all our patients were from a region with low HPV infection and that the present study was performed using recent cases (2006–2009).

Characteristic histopathology of HPV-related cancers has been reported, with differentiation grades appearing to differ depending on the site. For example, HPV-related SCC in the lung are mostly well differentiated,[48] half of all uterine cervical cancers are moderately differentiated,[49,50] and tonsillar SCC are poorly differentiated.[29,30] Unfortunately, the relatively low number of cases in the present study means that we did not have a sufficiently wide enough spectrum of differentiation (e.g. we only had two cases of poorly differentiated tumors and no NK SCC cases) and so we cannot draw any conclusions about the histopathology of HPV-related MTC. However, it should be kept in mind that the subclassification of SCC used in the present study was derived originally from 89 tonsillar cancers and that there is a basic histological difference between the mobile tongue and the tonsil. In fact, the mobile tongue is covered by keratinized squamous epithelium, whereas the tonsil is coated with stratified, non-keratinized squamous epithelium. Thus, a subclassification system based on squamous cell maturation (i.e. keratinization) may not be suitable for classifying MTC.

Sexual behavior may be another factor affecting the prevalence of HPV. A higher number of lifetime sexual partners and engaging in oral sex are principal risk factors for exposure to HPV. In fact, several studies have reported increased risks of oral and oropharyngeal cancers among individuals with a high number of sexual partners.[9,42,43,51,52] Unfortunately, we cannot comment on the relationship between HPV infection in MTC in terms of sexual behavior in the present study because there are no data available. In terms of the impact of sexual behavior, notably that oral sex is a predominant cause of increased rates of MTC, a possible drawback of the present study is that only three of the 32 patients were women. There may be a greater correlation between MTC and HPV in women than in men because the issue of oral sex may be more relevant in the case of women.

Overexpression (1+ to 4+) of $p16^{INK4a}$ protein was observed in six of 32 patients (19%) of MTC. Integration of HPV to host cells leads to increased expression of oncogenes *E6* and *E7*. The HPV E6 and E7 proteins bind and functionally inhibit p53 and retinoblastoma protein (pRb), respectively, and the functional inactivation of pRb by E7 leads to upregulation of $p16^{INK4a}$ protein as a result of the loss of negative feedback control.[53,54]

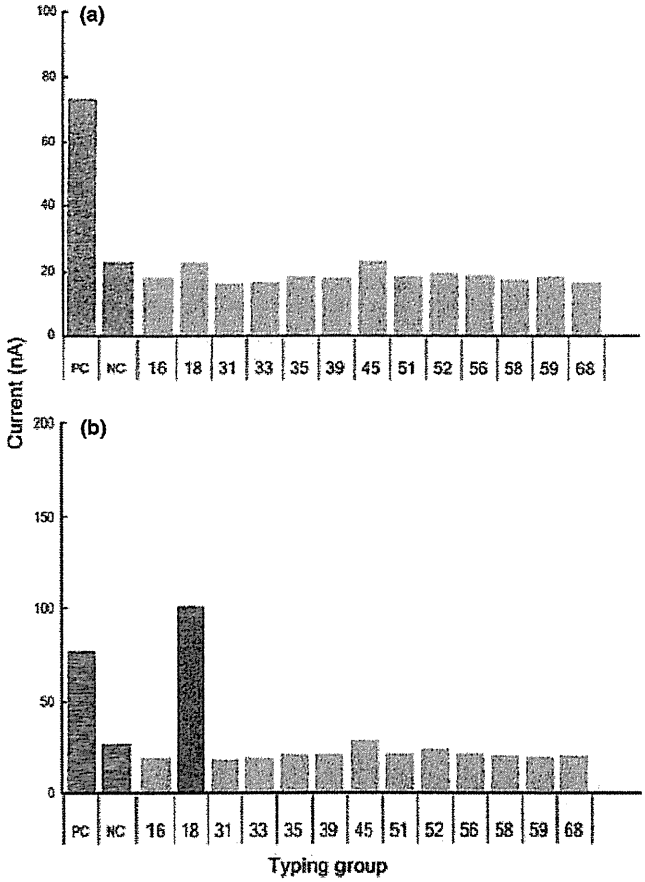

Fig. 3. Presence of high-risk human papillomavirus (HPV), as determined using a novel HPV DNA genotyping system with an electrochemical DNA chip and loop-mediated isothermal amplification (LAMP). Lane numbers correspond to HPV genotypes. PC, positive control; NC, negative control. (a) Patient 1 (see Table 2) was negative for all HPV genotypes. (b) A positive control sample (HPV genotype 18, cervical cancer, DNA extracted from paraffin-embedded block).

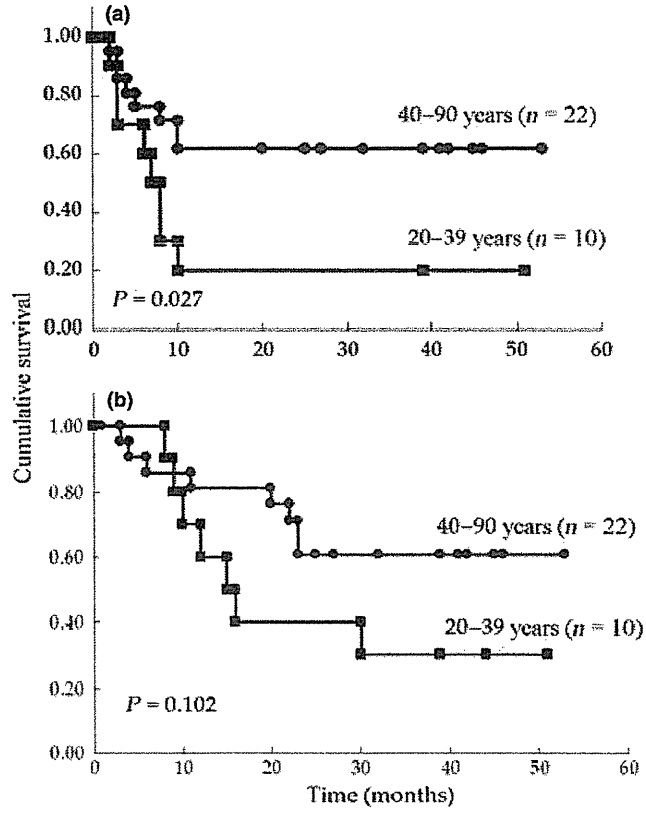

Fig. 4. Kaplan–Meier survival curves for (a) disease-free survival and (b) overall survival in younger (20–39 years) and older (40–90 years) patients. Both disease-free and overall survival analyses indicated a tendency for a less favorable prognosis in younger compared with older patients. However, the difference only reached statistical significance in the case of disease-free survival (log-rank test).

Thus, both overexpression of $p16^{INK4a}$ protein and lack of expression of p53 are usually evidence of an HPV-associated cancer.[28,55,56] However, in the present study, four of six tumors (67%) with $p16^{INK4a}$ overexpression also exhibited p53 overexpression. This suggests that the $p16^{INK4a}$ overexpression in these tumors bears little relation to HPV. It is true that overexpression of $p16^{INK4a}$ protein is a biomarker for cervical or tonsillar cancer arising from carcinogenic HPV infection,[30,33,57,58] but this is not the case for MTC.

The incidence of MTC among young adults is reported to be increasing, but this cannot be explained by ordinary carcinogens for oral cancer, such as smoking and alcohol consumption, because young people must have less cumulative exposure to carcinogens than older people.[21,59,60] It has been suggested that the increased HPV infection in industrialized countries was due, in part, to changing sexual behavior and an increase in oral sex.[61,62] This may be a cause of increased MTC, but are only few studies have investigated MTC in young patients, especially those in their 20s (Table 3). In the present study there were no HPV-positive cases in the six patients aged in their 20s or in the 10 young adults (20–39 years old). On the basis of these results, it is unlikely that HPV infection is a cause of increased MTC

Table 3. Human papillomavirus prevalence in mobile tongue cancer among young patients (<45 years of age)

References	Detection technique	Age (years)	Detection rate	Sample storage
Cruz *et al.*[16]	PCR	37, 39	2/2	FF
Liang *et al.*[11]	PCR	<45	1/8	FF
O'Regan *et al.*[20]	PCR	31, 33, 33, 37, 39, 39	HPV16 DNA 2/6 HPV16 E6/E7 mRNA 0/6	FF+PE
Cao *et al.*[18]	PCR	31, 38, 40, 42, 44	3/5	PE
Premoli-de-Percoco *et al.*[15]	PCR	29, 31, 32, 35, 40	5/5	FF
Siebers *et al.*[14]	ISH, PCR	23, 37	0/2	PE
Present study	ISH, GS*	21, 25, 26, 27, 28, 28, 31, 33, 35, 38, 44	0/11	FF

*The genotyping system (GS) used in the present study is a novel tool to detect 13 types of high-risk human papillomavirus (HPV) strains using electrochemical technology and loop-mediated isothermal amplification (LAMP). FF, fresh-frozen; PE, paraffin-embedded; ISH, *in situ* hybridization; PCR, polymerase chain reaction.

doi: 10.1111/j.1349-7006.2011.02149.x